JOURNAL OF GEOPHYSICAL RESEARCH, VOL. 104, NO. B4, PAGES 7463–7480, APRIL 10, 1999

Wide-angle seismic transect across the Torngat Orogen, northern Labrador: Evidence for a Proterozoic crustal root

Thomas Funck and Keith E. Louden

Department of Oceanography, Dalhousie University, Halifax, Nova Scotia, Canada

Abstract. A refraction/wide-angle reflection seismic transect across the Labrador peninsula covers the Core Zone of the SE Churchill Province, the Paleoproterozoic Torngat Orogen, and the Archean Nain Province including a portion of the Labrador continental margin. An airgun array was used as source, and 11 ocean-bottom seismometers and 16 land stations recorded the shots. Forward modeling of travel times and amplitudes reveals a deep asymmetric crustal root beneath the Torngat Orogen, with a crustal thickness of >49 km and with *P*-wave velocities of 6.9-7.0 km/s. The geometry of the velocity model and the root can be best explained by either westward dipping subduction or westward underthrusting of the Nain crust. Gravity modeling suggests a correlation of the crustal root with a gravity low that extends ~100 km in an E-W direction and ~200 km from north to south. The preservation of the crustal root is attributed to the lack of postorogenic heating and ductile reworking consistent with the lack of abundant postcollisional magmatism in the SE Churchill Province. A discontinuity possibly cutting through the entire crust is interpreted as a zone of major transcurrent shearing associated with the main phase of deformation. West of the Torngat Orogen, the crustal thickness in the Core Zone of the Churchill Province varies between 35 and 38 km (*P*-wave velocities of 5.8-7.0 km/s). East of the orogen, the crystalline crust in the Nain Province is ~38 km thick (velocities from 5.8 to 6.9 km/s) but thins to 9 km in the shelf area of the Labrador margin, where it is covered with up to 8 km of sediments. No high-velocity zone was found beneath the thinned continental crust at the margin.

1. Introduction

The geology in the northeastern Canadian shield (Figure 1) studied by the Lithoprobe Eastern Canadian Shield Onshore-Offshore Transect (ECSOOT) is characterized by a block of mainly Archean crust (Core Zone), which was trapped during the oblique convergence of the Archean Superior and Nain provinces [*Wardle and Van Kranendonk*, 1996]. The Proterozoic New Quebec Orogen sutures the Superior Province and the Core Zone to the west, while the Torngat Orogen sutures the Core Zone with the Nain Province to the east. The refraction/wide-angle seismic (R/WAR) transect across the Torngat Orogen was designed to address several questions associated with the development and structure of that orogen.

One major question is the crustal thickness beneath the Torngat Orogen. Seismic studies in associated Proterozoic orogens (e.g., the Trans-Hudson Orogen [*Lucas et al.*, 1993] and in the Baltic shield [*BABEL Working Group*, 1990]) reveal crustal roots, although such features are regarded as rather unusual for early Proterozoic orogens [*Wilson*, 1966]. The maintenance of the Torngat mountains as a relatively high mountain range (the peaks exceed 1700 m) over 1.8 Gyr and an associated Bouguer gravity low led to the idea that a crustal root might be preserved beneath the orogen. However, a reflection seismic survey across the northern Torngat Orogen [*Hall et al.*, 1995] did not show evidence for a crustal root. Our experiment is a transect across the southern Torngat Orogen designed to cross the gravity low and the mountain range to obtain a more definitive answer to the issue of a possible crustal root.

Previous geological studies and geodynamic models for the Torngat Orogen (e.g., the summaries by *Wardle and Van Kranendonk* [1996] and *Rivers et al.* [1996]) suggest a different evolution for the northern and southern Torngat Orogen. While eastward dipping subduction is well established in the north, there are different models for the south. It is fairly certain that early subduction in the southern Torngats was to the east, but there are several possibilities for its later development, including continued eastward subduction, double subduction, and flip of subduction direction [*Wardle and Van Kranendonk*, 1996]. The velocity model along the transect was not expected to give a final answer to these different geological models but instead to provide constraints for assessing crustal geometries predicted by the individual models.

Finally, there is surface evidence that transcurrent shearing is a major feature of the later stages of the Torngat Orogen. So far, it is unknown whether these shear zones sole within the crust or extend down to the mantle. A previous wide-angle seismic velocity model in the Nain Province [*Funck and Louden*, 1998] found evidence that a surface fault (Handy fault) is associated with a velocity contrast that cuts through

Paper number 1999JB900010.
0148-0227/99/1999JB900010$09.00

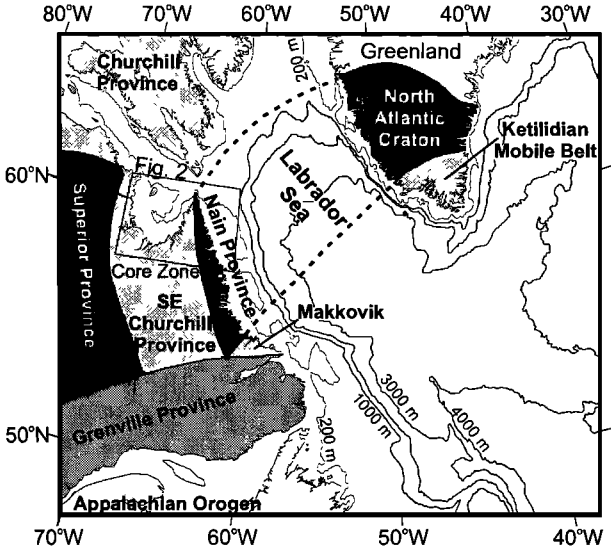

Figure 1. Tectonic provinces in the eastern Canadian shield and Greenland. The contour interval of the bathymetry is 1000 m. In addition, the 200-m-depth contour is plotted to show the approximate width of the shelf. A detailed tectonic map of the study area is shown in Figure 2.

the entire crust. The E-W transect reported in the present paper offers the opportunity to determine if similar deep velocity contrasts are also associated with one of the major shear zones (the Abloviak shear zone).

2. Geological Setting

The Paleoproterozoic orogenic development in the northeastern Canadian shield (Figure 1) was controlled by oblique convergence of the Archean Nain (North Atlantic) and Superior cratons [*Wardle and Van Kranendonk*, 1996], between which was trapped a belt of Archean gneiss (Core Zone). The New Quebec Orogen is situated between the Superior Province and the Core Zone to the west, and the Torngat Orogen is located between the Core Zone and the Nain Province in the east (Figure 2). Geological units across the E-W transect across the two orogens are briefly described below.

At the western end of the transect, the New Quebec Orogen is composed of low-grade continental margin rocks situated in a west verging fold and thrust belt, which is underlain by Superior Province basement [*Wares and Goutier*, 1990]. The eastern part of the orogen is overthrust by the

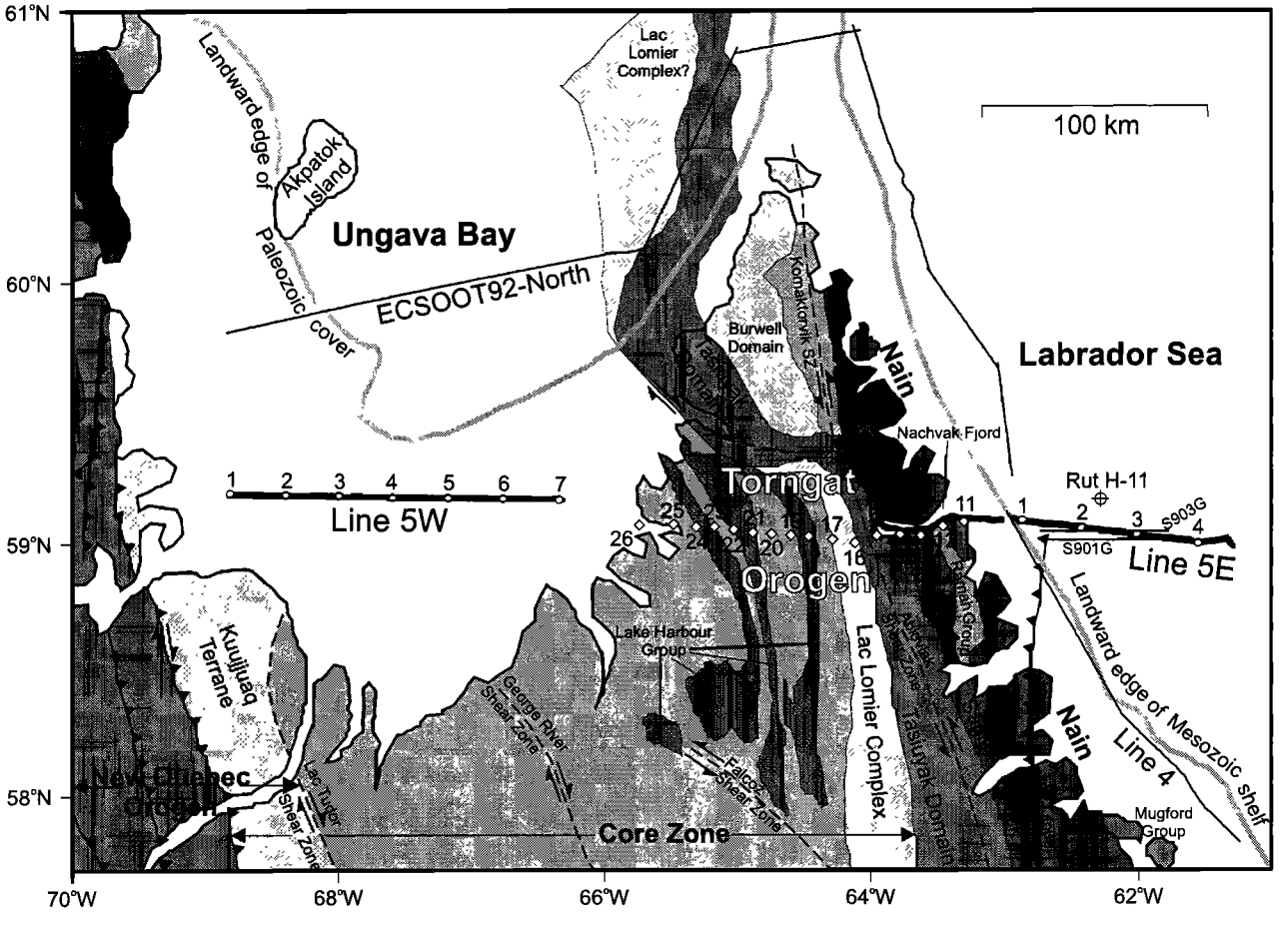

Figure 2. Tectonic map of the study area after *Hall et al.* [1995], showing the location of the transect (lines 5W and 5E). Solid bold lines show the segments with airgun-shots; circles and diamonds indicate the location of ocean bottom seismographs and seismic land stations, respectively. Thin solid lines show the location of other seismic profiles relevant to this study, as mentioned in the text. Solid lines with triangles mark faults and thrusts, dashed lines show shear zones (SZ), and arrows indicate the sense of displacement.

Kuujjuaq terrane, which consists of Archean gneisses [*Perreault and Hynes*, 1990].

The Core Zone of the southeastern Churchill Province is regarded as a composite zone [*James et al*, 1996] that in the west comprises Superior Province crust and in the interior comprises Archean rocks (dominantly orthogneisses) that are overlain locally by Paleoproterozoic metasedimentary rocks and intruded by 1.84-1.83 Ga [*Dunphy and Skulski*, 1995] arc-type plutons. Structures are generally west verging [*Goulet and Ciesielski*, 1990]. Several major vertical NNW-SSE trending shear belts in the Core Zone vary in sense from dextral in the west to sinistral in the east. In the northeast, the gneisses of the Core Zone are infolded with rocks of the Lake Harbour group, which is interpreted as a Paleoproterozoic cover sequence of shallow water origin [*Jackson and Taylor*, 1972].

The Torngat Orogen has four principal lithotectonic components (Figure 2) [*Wardle and Van Kranendonk*, 1996]: the Lac Lomier complex, the Tasiuyak domain, the plutonic suite in the Burwell domain, and the part of the Nain Province craton lying within the Torngat foreland (Four Peaks domain). The Lac Lomier complex is structurally overlain by the metasedimentary gneisses of the Tasiuyak domain, which is interpreted as the high-grade remnants of an approximately 1.9 Ga accretionary prism/arc complex [*Van Kranendonk et al.*, 1994]. The granitoid plutons of the Lac Lomier complex and the Burwell domain are interpreted as the roots of a 1.91-1.88 Ga magmatic arc system [*Ermanovics and Van Kranendonk*, 1990; *Bertrand et al*, 1993; *Van Kranendonk et al.*, 1994]. The structure of the orogen is characterized by outward verging thrusts and folds centered on the vertical Abloviak and Komaktorvik shear zones, which developed through sinistral shear. Torngat deformation commenced approximately 1.86 Ga, but the main episode of granulite-facies deformation and metamorphism occurred in association with the sinistral shearing approximately 1.845-1.82 Ga [*Bertrand et al.*, 1993; *Van Kranendonk*, 1996; *Rivers et al.*, 1996]. This event was simultaneous with the collision along the Superior-Core Zone and Core Zone-Nain boundaries. The Four Peaks domain in the foreland zone of the Torngat Orogen is underlain by Archean gneisses of the Nain Province [*Bridgwater and Wardle*, 1992].

The Nain Province on the eastern part of the transect is part of the North Atlantic craton (NAC) and can be correlated with the Archean block in southern Greenland [*Sutton et al.*, 1972; *Bridgwater et al.*, 1973; *Bridgwater and Schiøtte*, 1991]. The NAC has been a continuous structure prior to the Mesozoic rifting [*Srivastava*, 1978] that created the Labrador Sea between North America and Greenland.

3. Two-Dimensional Seismic Modeling

3.1. Experimental Layout and Data Processing

Line 5 of the ECSOOT R/WAR experiment is a 432-km long E-W transect across the northern tip of the Labrador peninsula, covering the Core Zone of the SE Churchill Province, the Torngat Orogen, and the Nain Province (Figure 2). The transect was split up in two segments along which CSS *Hudson* fired an array of six airguns (16.4 L each): (1) The western section (line 5W) consists of a 140-km line across Ungava Bay, with an average shot spacing of 125 m. (2) The eastern section (line 5E) consists of a 157-km segment (line 5E) with an average shot spacing of 135 m. Line 5E covers a 40-km segment of the Nachvak Fjord and extends across the shelf into the Labrador Sea. Shots from lines 5W and 5E were recorded by a set of 16 Reftek land seismographs (three-component 4.5-Hz geophones, average spacing 9 km) deployed across the Torngat Orogen between the shot lines. In addition, shots on line 5W were recorded on seven ocean bottom seismographs (OBS) from the Geological Survey of Canada (hydrophone and 4.5-Hz vertical geophone, average spacing of 23 km), and those on line 5E were recorded by four OBS (average spacing 25 km).

Water depths along line 5 vary between 30 and 220 m. Shot-receiver ranges were computed from the ship's Global Positioning System (GPS) and land differential GPS navigation. The seismic data were coherency mixed across five traces using the method of *Chian and Louden* [1992], followed by a band-pass filter (4 to 10-Hz land stations, 5 to 9-Hz OBS). The record sections (Figures 3-11) are displayed with a reduction velocity of 7.5 km/s, and individual traces are normalized by their RMS amplitude.

3.2. Methodology

For the setup of the model, all receivers were projected on a straight line connecting the western and eastern limits of line 5. The average offset of the stations from this line is 5.5 km. This is not critical to the modeling since the main tectonic features strike in north-south direction, perpendicular to the line. For the modeling of land stations (average elevation 306 m), all of which were deployed on basement, travel time picks were corrected to sea level, using a basement velocity of 6.0 km/s.

To determine the velocity structure of the crust and upper mantle along line 5, the programs RAYINVR and TRAMP [*Zelt and Ellis*, 1988; *Zelt and Smith*, 1992; *Zelt and Forsyth*, 1994] were used. The first step was the forward modeling of travel times. The data required a water layer, three sedimentary layers, three crustal layers, and a layer for the upper mantle. The spacing of the velocity and depth nodes was originally 25 km. However, around some complex features (e.g., faults), the node spacing was later reduced to ~5 km. After generating a basic model, the amplitude information of the records was incorporated in the forward modeling to achieve the best possible fit for both amplitudes and travel times. The amplitude modeling was based on the computation of ray-theoretical synthetic seismograms and a qualitative comparison with the field records. Gaussian random noise has been added to the synthetic seismograms in Figures 3-5 to match the signal-to-noise ratio of the original record sections. The source wavelet for the seismograms was extracted from a record trace and includes the reverberations caused by the untuned airgun array used for the shooting.

3.3. R/WAR Data

P-wave records on line 5 include P_g, P_c, and P_n corresponding to refractions in the upper/middle crust, lower crust, and upper mantle, respectively; P_cP and P_mP are reflections from the middle- to lower-crustal boundary and the Moho. Two OBS on line 5W recorded a crustal reflection from the upper-/middle-crust boundary, named P_rP. In the eastern part of the line, refractions from three sedimentary layers (P_{S1},

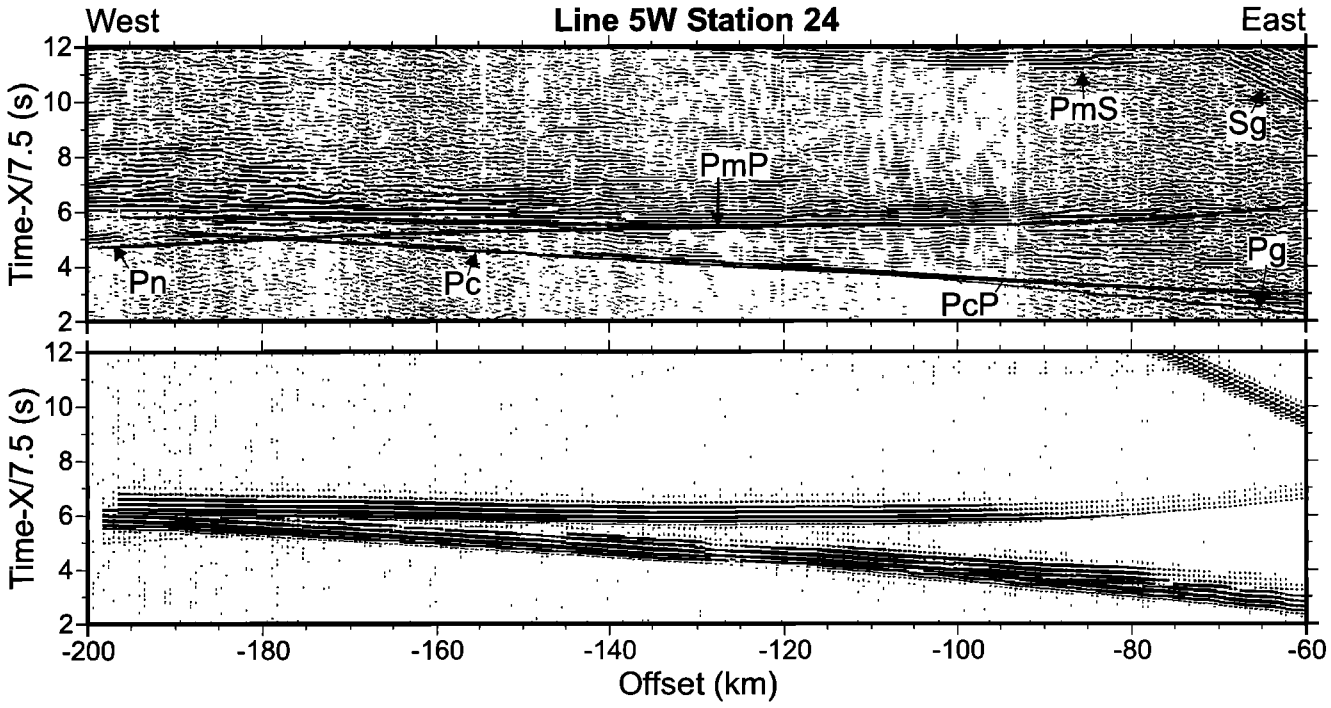

Figure 3. Record section with (top) computed travel times and (bottom) synthetic seismogram for station 24 on line 5W. Horizontal scale is the shot-receiver distance, and vertical scale is the travel time using a reduction velocity of 7.5 km/s. Processing includes coherency mix (five traces, 5.0-8.5 km/s), band-pass filter (4-10 Hz), and trace normalization. See text for description of phases.

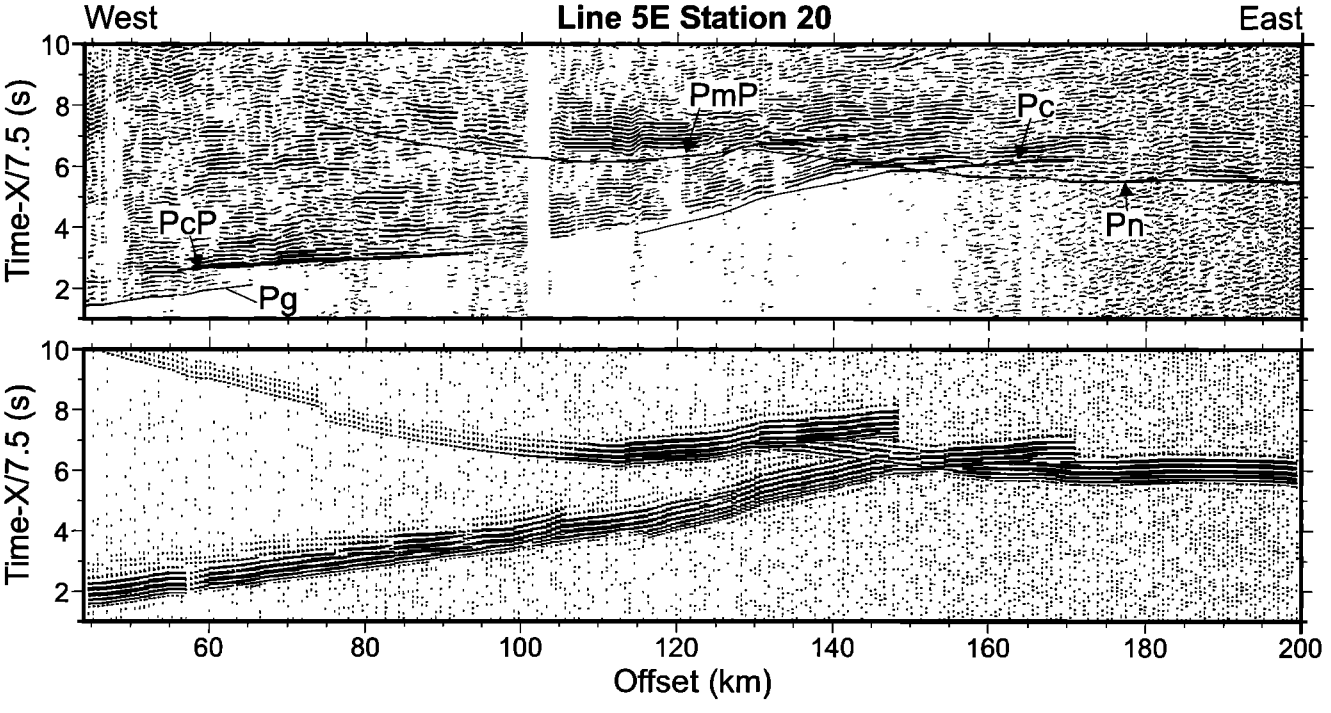

Figure 4. Record section with (top) computed travel times and (bottom) synthetic seismogram for station 20 on line 5E. Horizontal scale is the shot-receiver distance, and vertical scale is the travel time using a reduction velocity of 7.5 km/s. Processing includes coherency mix (five traces, 5.0-8.5 km/s), band-pass filter (4-10 Hz), and trace normalization. See text for description of phases.

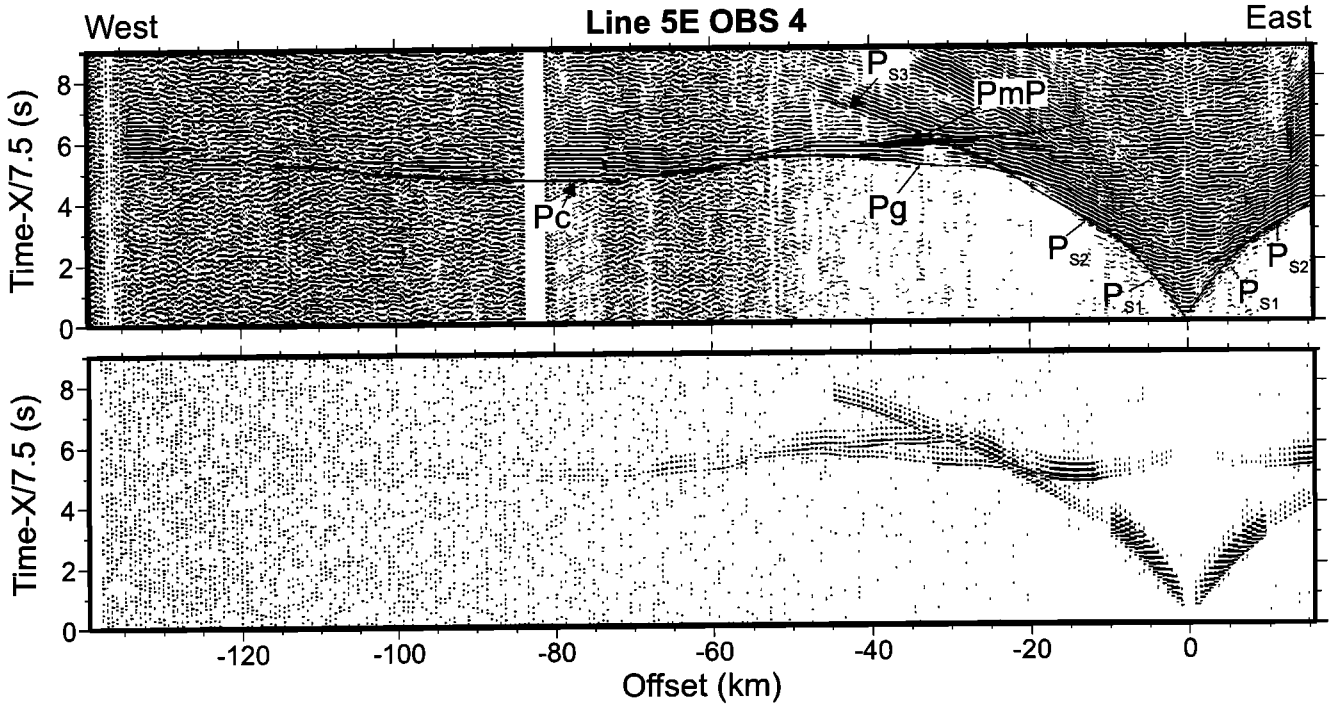

Figure 5. Record section with (top) computed travel-times and (bottom) synthetic seismogram for OBS 4 on line 5E (hydrophone). Horizontal scale is the shot-receiver distance, and vertical scale is the travel time using a reduction velocity of 7.5 km/s. Processing includes coherency mix (five traces, 5.0-8.5 km/s), band-pass filter (5-9 Hz), and trace normalization. See text for description of phases.

P_{S2}, and P_{S3}) were observed. Some records also show *S*-wave arrivals (e.g., the refraction in the upper crust, S_g, in Figure 3) and *P*-to-*S* conversions at the Moho (P_mS, Figure 3). *S*-phases were not modeled in this study. In the remainder of this paper, the term "offset" will refer to the range between shot and receiver (positive to the east), and "distance" will give the location along the line relative to the westernmost shotpoint as 0 km.

Data quality for the land stations on both lines 5E and 5W and OBS on line 5E generally is good. In contrast, the quality of OBS recordings on line 5W is only poor to moderate; the maximum offset to which arrivals can be correlated varies between 20 and 70 km. We attribute the lower data quality on western OBS to strong tidal currents in the shallow water of Ungava Bay, introducing a high noise level. These currents were also a problem during the ECSOOT 1992 reflection seismic experiment [*Hall et al.*, 1995].

Further inspection of the record sections allows us to distinguish between three typical sections comprising line 5W land stations, line 5E land stations, and line 5E OBS. One example for each of these types is briefly described below.

1. Records from line 5W are good examples of a simple and horizontally homogeneous velocity structure with very distinctive phases that can be correlated well across large distances. On station 24 (Figure 3), the P_mP phase can be correlated with high amplitudes between offsets from -80 to -200 km. First arrivals are marked by the crustal P_g phase (velocity 6.0 km/s) and P_c phase (velocity 6.4 km/s), with crossover to P_n phase (velocity 8.8 km/s) at an offset of -175 km. The midcrustal reflection (P_cP) appears weakly at around -100 km. The general consistency and simplicity of the arrivals from station to station indicates a rather uniform structure in the western part of line 5.

2. Landstations observing arrivals from line 5E (Figure 4) are characterized by strong P_mP phases, but the arrival times show significant undulations and the overall patterns of this phase are more diffuse and complex than on line 5W. Modeling shows that these features are caused by the crustal thinning and sediment infill at the Labrador continental margin. Refracted crustal phases (P_g and P_c) are normally strong arrivals that are delayed in the eastern part of line 5E by the sediment infill, as indicated by the decrease of the apparent P_g velocity from 5.6 to 4.9 km/s at 114-km offset on station 20 (Figure 4). At 145 km, the P_g phase crosses over into the P_c phase (velocity 6.3 km/s), and at 150 km the P_n phase (velocity 8.1 km/s) takes the place of the P_c phase as the first arrival. A midcrustal reflection (P_cP) is clearly recognizable between offsets of 55-85 km.

3. OBS 2-4 on line 5E are marked by a pronounced delay of the crustal phases due to the thick sediment sequences. OBS 4 (Figure 5) shows three refracted phases in the sediments (P_{S1}, P_{S2}, and P_{S3}) with phase velocities of 2.2, 3.4, and 4.3 km/s, respectively. The P_g branch becomes the first arrival at an offset of -23 km with a phase velocity of 6.0 km/s. The phase velocity of the P_c phase west of -50 km undulates between 7.0 and 9.1 km/s. The postcritical P_mP phase can be seen at an offset of -32 km, indicating a fairly thin crust in the easternmost section of the line.

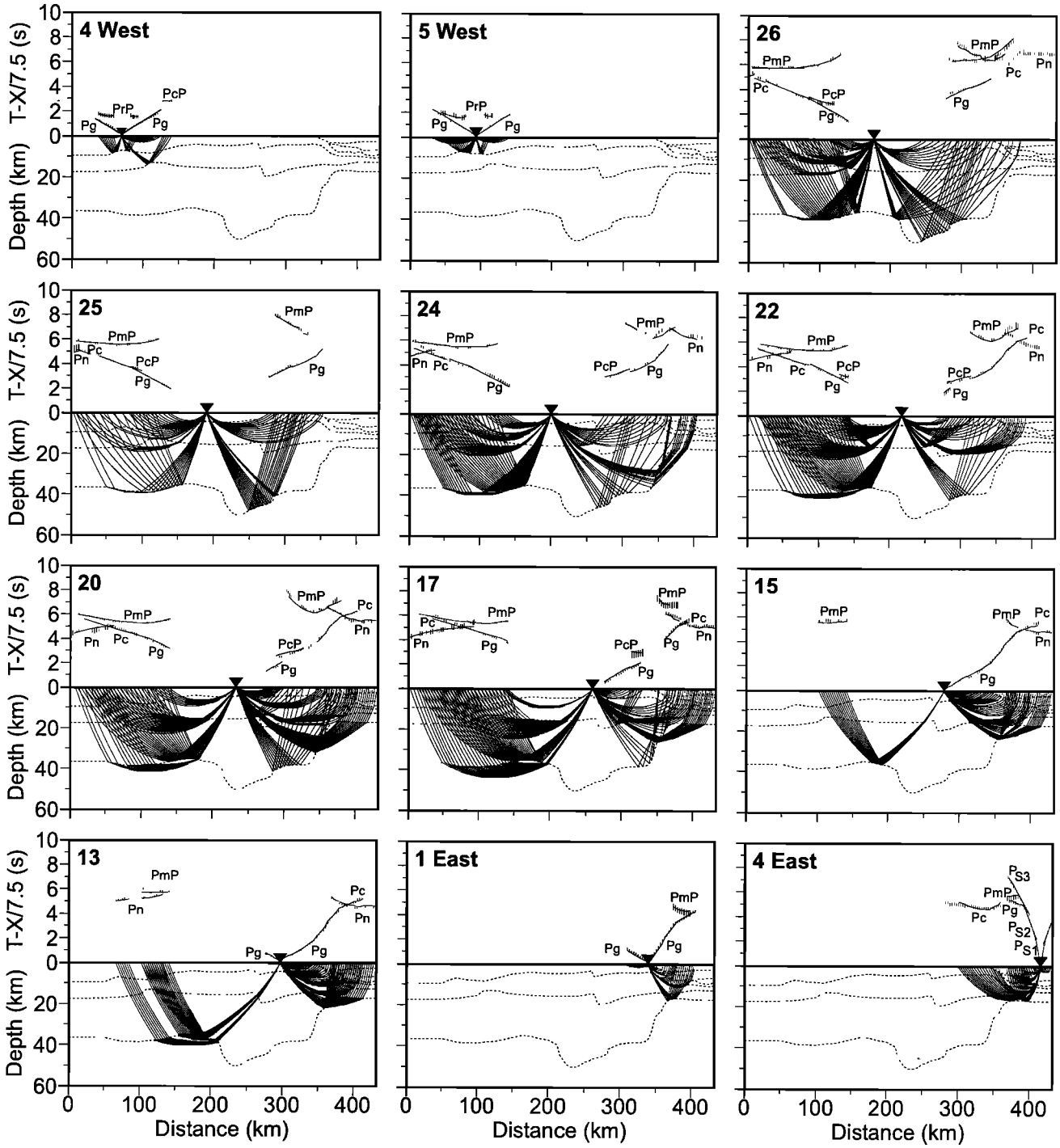

Figure 6. Comparison of observed and calculated travel times for a selection of 12 stations (from a total of 27 stations) along the transect, shown together with the corresponding ray paths. Observed data are indicated by vertical bars, with heights representing pick uncertainty; calculated data are indicated by solid lines. Triangles mark the receiver location. Horizontal scale is the model position; a reduction velocity of 7.5 km/s has been applied for the travel times.

4. Results

The fits of calculated to observed travel times are shown in Figure 6 for a selection of stations along line 5. Before the final velocity model is presented in detail, certain of its relevant features are discussed in terms of the seismic constraints on them. The total constraint on individual features in the model is more extensive than can be summarized in a single figure. We have chosen the most suitable seismograms to illustrate the observations described in the text, but neighboring stations also have contributed to the final crustal velocity model.

4.1. Continental Margin Sediments

The sedimentary sequence on the margin causes noticeable delay times of the crustal phases (Figures 4 and 5). A good model for the sediments is therefore crucial before proceeding with the modeling of deeper crustal layers. In addition to the

OBS along line 5E, several other data sets have been integrated into the model. The onset of thicker sediment layers in the model of line 5 is consistent with the landward edge of the Mesozoic shelf (Figure 2) as mapped from a compilation of reflection seismic profiles along the continental margin (J. Hall, personal communication, 1995). The seaward thickening of the sediments up to a distance of 375 km was taken from two commercial reflection seismic lines (lines S901G and S903G from Total Eastcan Exploration Ltd.; Figure 2). The two-way travel times were converted to depth using the velocity log from a nearby drill site (Rut H-11, Petro Canada Exploration Inc.; Figure 2) down to 4075 m. Farther seaward, the basement lies outside the recording window of the reflection lines and the lower sediments were modeled by the refraction data from line 5E. The internal division of the sediments into three subunits with velocities of 2.0-3.2, 3.4-3.9, and 3.8-4.3 km/s, respectively, is based on the OBS data. Average velocities in the model to depths of 4 km are compatible with measurements at the drill site within a range of ±0.2 km/s.

4.2. Upper Crustal Reflector

The crust along line 5 is subdivided into three layers: upper, middle, and lower crust. The transition from the upper to the middle crust is in general associated with a reduction of the velocity gradient without a velocity discontinuity. However, two stations on line 5W (OBS 4 and 5) show a reflection (P_rP) from upper- to middle-crustal depths. Figure 7 shows the P_rP phase recorded by OBS 5. The P_rP phase is quite distinguishable before it interferes with the P_g phase. Mapping of the reflection points of the P_rP phase yields a lateral extent of a reflective upper-/middle-crust boundary from 55 to 105 km at a depth of about 8 km. For the remainder of line 5W the data were too noisy to identify possible P_rP arrivals.

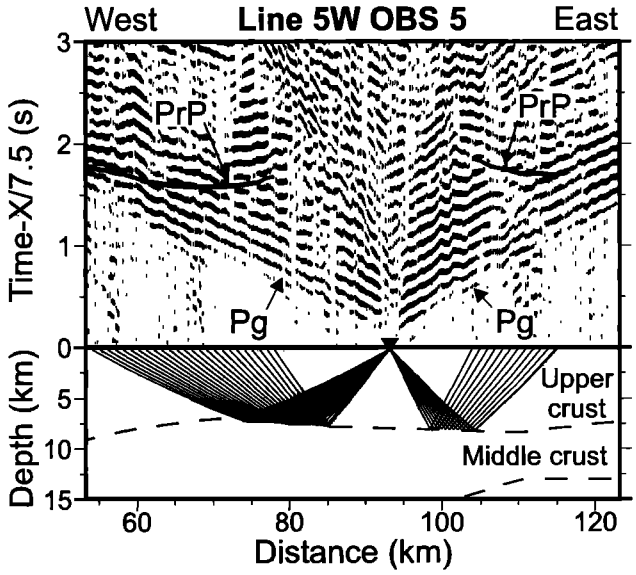

Figure 7. (top) Close-up view of record section for OBS 5 on line 5W overlain with the computed travel times for the P_rP phase (reflection at the base from the upper crust) as shown in (bottom) the corresponding ray path diagram. The triangle marks the receiver position in the model. Horizontal scale is model position; a reduction velocity of 7.5 km/s has been applied for the travel times.

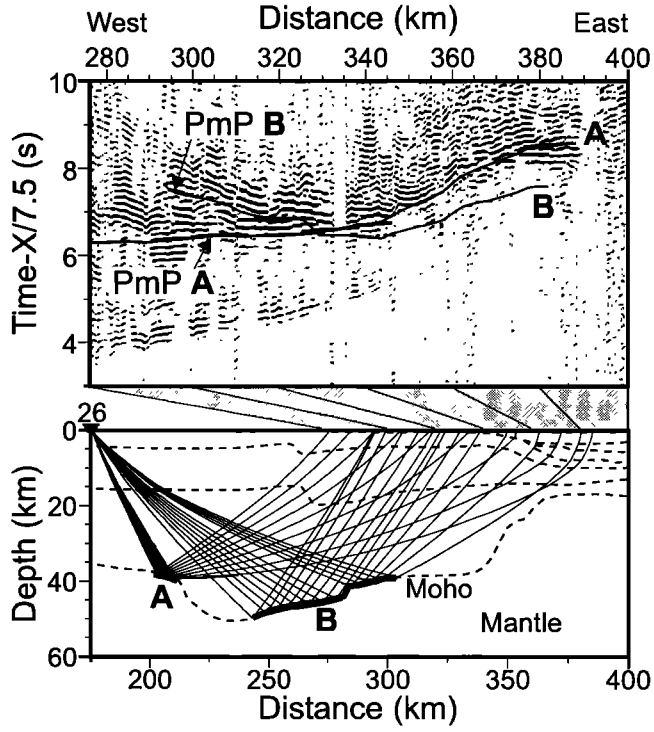

Figure 8. (top) Close-up view of record section for station 26 on line 5E overlain with the computed travel times for the P_mP phase (Moho reflection) as shown in (bottom) the corresponding ray path diagram. Letters A and B distinguish the P_mP phases reflected from the western border and from the eastern segment of the crustal root, respectively. The triangle marks the receiver position in the model. Horizontal scale is model position; a reduction velocity of 7.5 km/s has been applied for the travel times.

4.3. Crustal root

Between 210 and 285 km distance, Moho depth increases to a maximum of 50 km, forming a crustal root beneath the Torngat Orogen. The shape of the root results in complex P_mP reflection patterns with partly interfering reflection branches. The root is imaged by P_mP recordings from three stations (stations 24-26; Figure 6). Models for station 26 (Figure 8) show how the main characteristics of the root were determined. The western rim of the root is defined by P_mP reflections from the reflector element A. The sudden disappearance of the corresponding reflection branch A is modeled with an abrupt change of Moho depth at 210 km. Although the actual width of the reflector element A is only 10 km, the corresponding reflection can be correlated across more than 100 km. Between 295 and 330 km, another strong P_mP reflection (branch B) follows the first P_mP branch A, reflected from the deeper portion of the root east of 240 km. The Moho between 210 and 240 km distance is not imaged by reflections. There are however some limitations to possible configurations. The sudden appearance of strong P_mP amplitudes of branch B at 295 km indicates that this is the distance at which the reverse travel time branch (connecting A and B) terminates. At the western rim of the root, an abrupt increase in depth is required, as previously discussed. These requirements can be best fulfilled with a downward convex shape of the Moho. The absence of a reverse P_mP branch in the record section between A and B can be explained by two

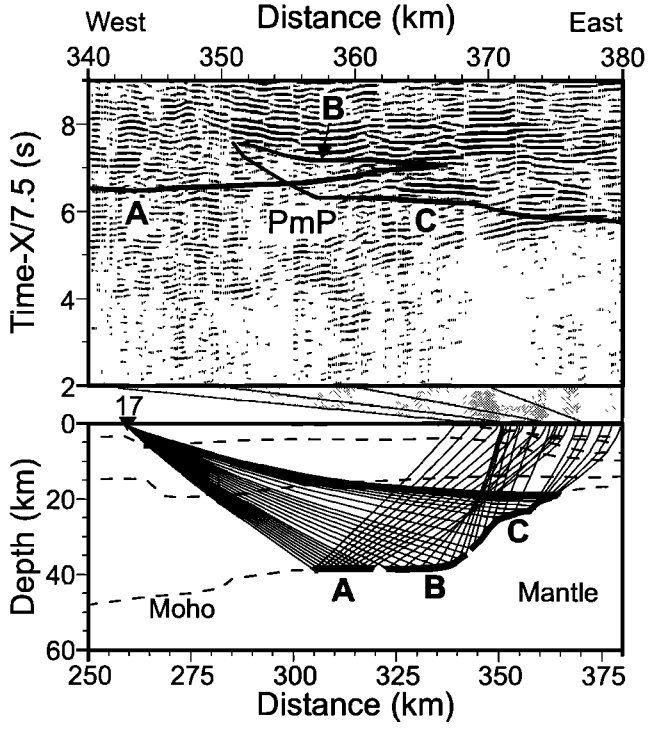

Figure 9. (top) Close-up view of record section for station 17 on line 5E overlain with the computed travel times for the P_mP phase (Moho reflection) as shown in (bottom) the corresponding raypath diagram. Letters A, B, and C distinguish the P_mP phases reflected from the different segments along the base of the thinning crust at the Labrador margin. The triangle marks the receiver position in the model. Horizontal scale is the model position; a reduction velocity of 7.5 km/s has been applied for the travel times.

processes. Either the arrivals are hidden in the reverberations and noise following the first arrivals, or the Moho between 210 and 240 km is a rather complex zone tending to weaken the P_mP amplitudes.

4.4. Crustal thinning

Toward the continental margin of Labrador, Moho depth shallows from 38 to 17 km. The transitional zone where the actual thinning occurs is again characterized by complex P_mP reflection patterns with interference of several reflection branches. Figure 9 shows an example for station 17 recording the shots of line 5E. Branch A from the Moho between 305 and 320 km defines the portion of the Moho that is west of the thinned crust. Reflector element B between 325 and 340 km is bent upward due to initiation of crustal thinning, resulting in the reverse P_mP branch B with strong reflection amplitudes. Reflector element C between 345 and 365 km comprises the portion with a maximum Moho dip of ~50°, followed by flattening to the east. The amplitude of the P_mP branch C increases to the east as the angle of incidence of the rays increases rapidly with the shallowing Moho.

4.5. Abloviak Shear Zone

The seismic model between 260 and 285 km is characterized by steps in the layer geometry at all crustal levels (Figures 10 and 11). These steps are arranged on a gradually eastward dipping line, interpreted to represent the downward continuation of the western border of the Abloviak shear zone. Most prominent in the records is the discontinuity for the midcrustal boundary (MCB), whose depth changes by about 5 km across the discontinuity. Figure 10 shows the change of the reflection patterns of the P_cP phase for stations 20 and 18. The P_cP phase recorded at station 20 is reflected west of the step at a depth of 15 km, while the reflection points for station 18 are to the east of the discontinuity at a depth of 20 km. Hence the P_cP phase at station 20 arrives earlier than at station 18 and with a lower phase velocity.

The necessity of a step at the boundary between upper and middle crust is not as easy to define as for the MCB, because no reflections are observed. However, there is a systematic change in the range of the high-amplitude P_g phase through the upper crust for stations in that region. The record section of station 20 (Figure 10a) shows that the P_g phase has only weak-to-moderate amplitudes for offsets less than 55 km. For larger offsets the phase fades out. In contrast, station 18 (Figure 10b) shows stronger amplitudes for the P_g phase to an offset of 62 km before fading out. The simplest way to model such a behavior of the P_g phase is by increasing the upper crustal thickness east of 260 km.

Moho depth changes by ~2 km across the discontinuity (Figure 11). Station 24 (Figure 11a) shows a good fit for the P_mP reflections A west of the step. Reflections B from the east of the discontinuity correspond to weaker P_mP phases east of 325 km in the record section. In contrast, station 22 (Figure 11b) shows a strong amplitude and a good fit for reflections B east of the step, while reflections A from the west are hardly visible. However, the transition between the P_mP branches A and B is more complex for both stations than suggested by the ray tracing. This probably causes some of the misfit in the transition region between branches A and B. However, the P_mP travel time misfit for the stations shown in Figure 11 and for the neighboring stations (stations 20-26) is minimized by changing Moho depths in the model at 285 km, although the depth change of 2 km is close to the limit of resolution.

Additional evidence for the discontinuity comes from analysis of the amplitudes of the record sections on line 5W. While stations 26-17 have a very high signal-to-noise ratio, only few arrivals can be correlated on stations 16-11. The transition from a high to a low signal-to-noise-ratio between stations 17 and 16 (Figure 12) coincides with the location of the modeled discontinuity, indicating that rays crossing the near-vertical trace of the shear zone are attenuated. The geometry along the discontinuity changes from west-side-up/east-side-down at the upper and middle crust to a reverse sense at the Moho. This is in agreement with the interpretation that the discontinuity is associated with a transcurrent component (shearing).

4.6. Final Velocity Model

The final velocity model is shown in Figure 13. The model can be subdivided into four sections for which the descriptions are given below, moving from the west to the east. The western part of the model between 0 and 210 km is characterized by an overall crustal thickness of 35-38 km. The upper crust thins from 9 km in the west to 4 km in the east, with velocities between 5.8 and 6.25 km/s. The transition between the upper and middle crust is normally associated with a

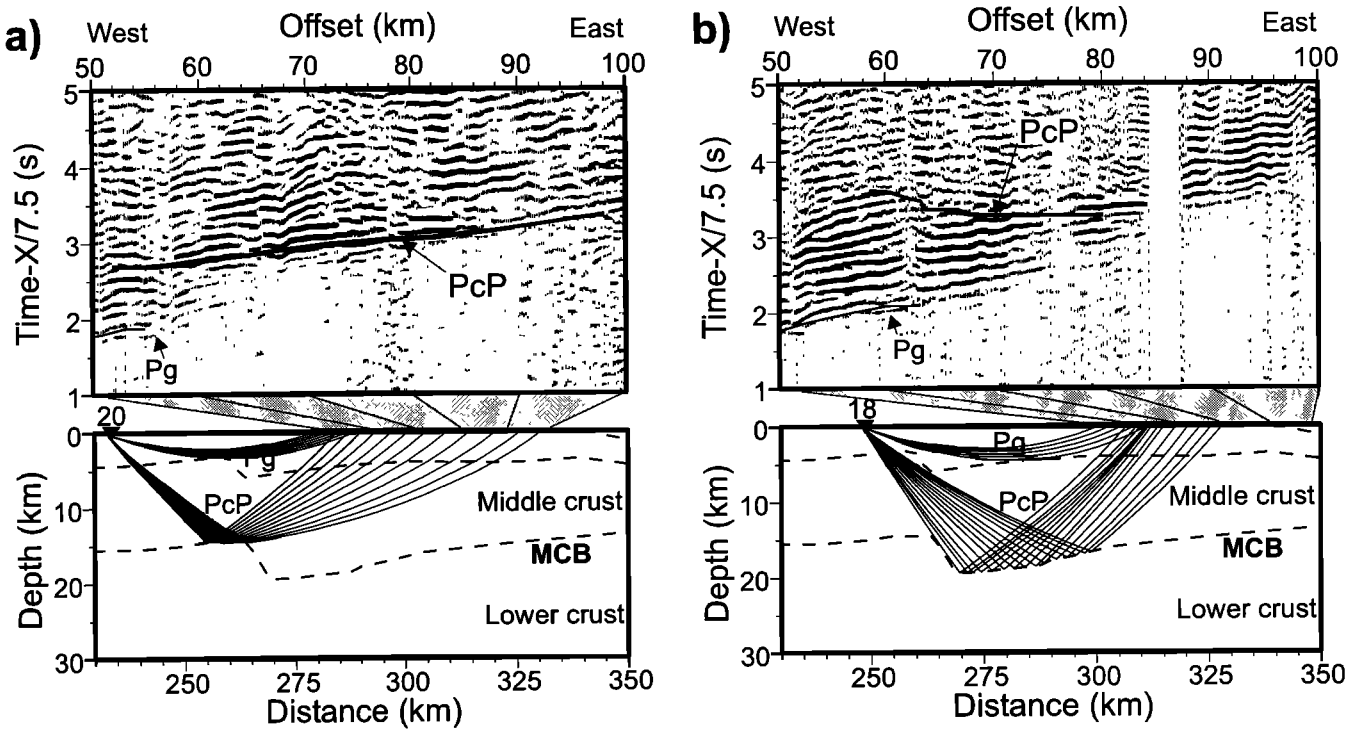

Figure 10. (top) Close-up view of record sections for (a) station 20 and (b) station 18 on line 5E overlain with the computed travel times for the P_g and P_cP phase as shown in (bottom) the corresponding ray path diagrams. The triangles mark the receiver positions in the model. Horizontal scale is the model position for the ray path diagram and shot-receiver distance for the record section; a reduction velocity of 7.5 km/s has been applied for the travel times. (MCB indicates midcrustal boundary.)

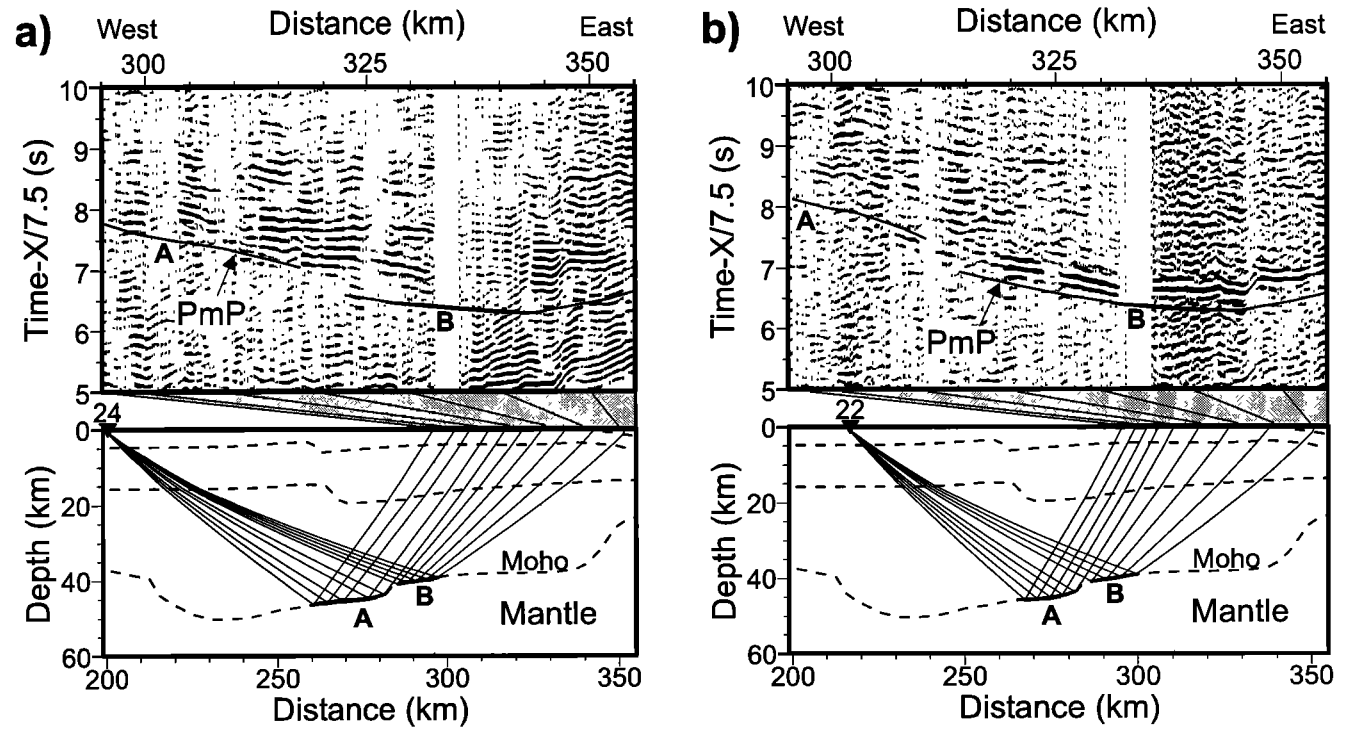

Figure 11. (top) Close-up view of record section for (a) station 24 and (b) station 22 on line 5E overlain with the computed travel times for the P_mP phase (Moho reflection) as shown in (bottom) the corresponding raypath diagram. Letters A and B distinguish the P_mP phases reflected from the west and from the east of the Moho step, respectively. The triangles mark the receiver positions in the model. Horizontal scale is the model position; a reduction velocity of 7.5 km/s has been applied for the travel times.

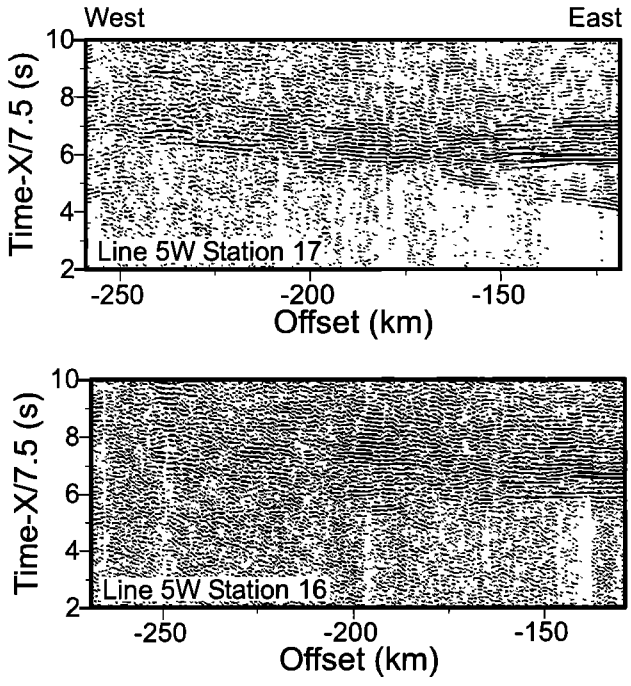

Figure 12. (top) Record section of station 17 and (bottom) station 16 on line 5W. Stations 17 and 16 are the closest stations to the west and east of the crustal discontinuity, respectively. Horizontal scale is the model position; a reduction velocity of 7.5 km/s has been applied for the travel times.

decrease in the velocity gradient without a velocity discontinuity. However, between 55 and 105 km the boundary is characterized by a velocity change of 0.1 km/s. Midcrustal velocities range between 6.1 and 6.45 km/s. The depth of the mid-crustal boundary (MCB) varies between 17 and 13 km, with a velocity increase of 0.1-0.15 km/s toward the lower crust. The lower crust is 19 to 22 km thick, and its velocities increase from 6.55 km/s at the MCB to 7.05 km/s at the Moho. A slight updoming of the structure at the upper-/middle-crust boundary occurs around 75 km and at the MCB at 120 km.

The crust beneath the Torngat Orogen from 210 to 285 km is characterized by an asymmetric crustal root with a maximum thickness of >49 km, with a steeper flank on the west than on the east. Upper- and middle-crustal levels are not affected by the thickening. A nearly vertical discontinuity at the border of a shear zone cuts through the entire crust between 260 and 285 km, dipping approximately 60° toward the east. Across this discontinuity, the depth of the upper-/middle-crust boundary increases by 2.5 km to the east and the MCB by 5 km, while the Moho rises by 2 km. The upper crust has a thickness of 4 km, with velocities between 5.9 and 6.1 km/s west of the discontinuity, while its thickness is 6 km to the east and the velocity reaches 6.2 km/s. West of the discontinuity, the middle crust is 11 km thick (velocity v=6.1-6.4 km/s); to the east it thickens to 14 km (v=6.2-6.55 km/s). Lower crustal velocities range from 6.6 to 6.9 km/s and up to 7.0 km/s in the deeper portion of the crustal root.

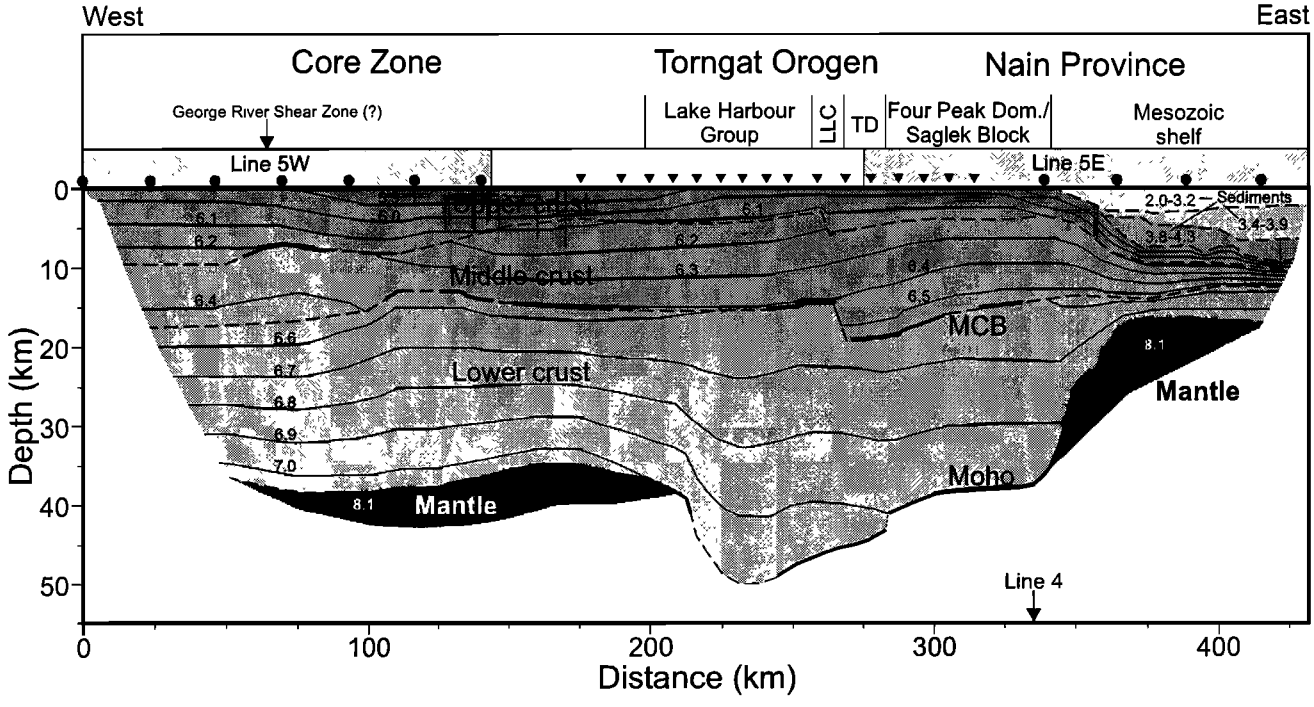

Figure 13. *P*-wave velocity model with a contour interval (thin solid lines) of 0.1 km/s in the crystalline crust and mantle. Numbers indicate velocity, in km/s. The outer perimeter of the model with no ray coverage is omitted. Layer boundaries are drawn with dashed lines where they are not constrained by reflections and with bold solid lines elsewhere. The arrow indicates the cross point with line 4 [*Funck and Louden*, 1998]. Gray boxes above the model show the segments with airgun shots; circles and triangles mark the location of OBS and land stations, respectively. Tectonic units are indicated in the uppermost box. Abbreviations are LLC, Lac Lomier complex; TD, Tasiuyak domain; and MCB, midcrustal boundary. Vertical exaggeration is 2.8.

Table 1. RMS Misfit Between Calculated and Picked Travel Times for Individual Phases and Shot Lines.

	Line 5W		Line 5E		Lines 5W and 5E	
Phase	n	t_{rms}, s	n	t_{rms}, s	n	t_{rms}, s
P_{S1}	0	-	48	0.148	48	0.148
P_{S2}	0	-	86	0.102	86	0.102
P_{S3}	0	-	39	0.079	39	0.079
P_g	688	0.108	1419	0.120	2107	0.116
P_rP	84	0.064	0	-	84	0.064
P_cP	314	0.084	222	0.171	536	0.127
P_c	525	0.142	333	0.123	858	0.135
P_mP	1452	0.117	516	0.144	1968	0.124
P_n	454	0.129	390	0.152	844	0.140
All phases	3517	0.117	3053	0.133	6570	0.125

The next crustal subsection extends from 285 to 338 km, corresponding to the relatively pristine Archean crust of the Nain Province. The Moho depth changes from 41 km in the west to 38 km farther east. The MCB flattens from 18 km near the discontinuity to 14 km in the east. Velocities in the 5-km-thick upper crust range from 5.9 to 6.2 km/s, in the middle crust range from 6.2 to 6.55 km/s, and in the lower crust range from 6.6 to 6.9 km/s.

The section east of 338 km corresponds to the Mesozoic margin with the Labrador Sea. At 338 km, thin sediments are first observed, coinciding with the onset of the crustal thinning. The sediment sequence is composed of three layers, with velocities of 2.0-3.2, 3.4-3.9, and 3.8-4.3 km/s, respectively. Their overall thickness increases relatively rapidly to 7.5 km between 350 and 375 km. From that point, they thicken slowly to 9 km at the eastern limit of the line. The thickness of the crystalline crust decreases from 38 km at a distance of 338 km to 9 km at 375 km. Farther to the east, Moho depth is constant at around 17 km. No internal crustal structure could be detected within the thinned crust. Crustal velocities range between 5.9 and 6.9 km/s where the thinning starts and between 5.8 to 6.75 km/s east of 375 km.

4.7. Model Resolution and Uncertainty

The final velocity model shows a good fit to the observed travel times (Figure 6), and the synthetic seismograms (Figures 3-5) match the record sections in a qualitative sense. To derive a more quantitative description of the fit, arrival time misfits were computed as summarized in Table 1. The average RMS misfit between observed and calculated travel times is 117 ms for shots on line 5W and 133 ms on line 5E. Part of this misfit has to be attributed to the uncertainty in arrival times, which varies between a minimum of 40 ms for good first arrivals and a maximum of 250 ms for noisy second arrivals.

Ray coverage on the western section is somewhat limited in terms of crossing ray paths because of the low signal-to-noise-ratio for the seven OBS on that line. Intersecting ray coverage was only achieved for the upper crust, whereas the middle and lower crusts are almost entirely defined by the 16 land stations to the east of line 5W. However, the close spacing of the land stations (9 km) can partly compensate for this limitation, providing a fairly consistent view of the deeper crustal levels that is also compatible with the gravity model (next section).

To determine the uncertainty of the velocity and boundary nodes, single nodes of the model were perturbed and the travel times were checked for their sensitivity to these variations. The uncertainty of crustal velocities was found in general to be ±0.1 km/s. However, two areas are associated with an uncertainty of ±0.15 km/s. These areas include the crust west of 75 km, with a lower ray coverage than in other areas, and the upper crust between 150 and 275 km, where the shooting gap between lines 5W and 5E results in lack of P_g observations through the upper crust. Upper mantle velocities where observed are certain to within ±0.1 km/s, and the individual sediment layers have an uncertainty of ±0.15 km/s. The outer perimeter of the ray coverage is included in Figure 13, and layer boundaries defined by reflections are marked by bold lines. Coverage of the Moho by P_mP reflections is fairly complete, with the exception of the western part of the crustal root between 210 and 240 km, as discussed above. The absence of P_mP arrivals from this segment suggests a convex downward shape of the Moho. In the remaining areas, the uncertainty of the Moho depth is of the order of 1 km. The MCB and the upper-/middle-crust boundary can be modeled within an uncertainty of ±1.5 km. All specified errors for layer velocities and boundary depths are given on the assumption that the remaining model parameters are correct.

4.8. Gravity Modeling

To check if the velocity model of line 5 is consistent with the gravity data, two-dimensional (2-D) gravity modeling was carried out. The gravity values along line 5 were sampled from a gravity grid for that area (Plate 1), computed from data of the Geological Survey of Canada (onshore and in the Labrador Sea) and from Geosat and ERS 1 satellite altimetry (version 7.2 released by D.T. Sandwell and W.H.F. Smith) in Ungava Bay. Bouguer anomalies are used for land areas, and free-air anomalies are used for offshore areas. The gray shading of the gravity map (Plate 1) is derived from illumination of magnetic data (Geological Survey of Canada) from the west.

The initial density model, with velocities converted to density by applying the empirical formula of *Ludwig et al.* [1970], showed large misfits of up to 110 mGal (Figure 14) in the eastern area corresponding to the thinned crust. Given the magnitude and wavelength of this offset, the main source for this misfit must lie in the mantle. As the misfit begins and increases with the thinning of the crust, the mantle was

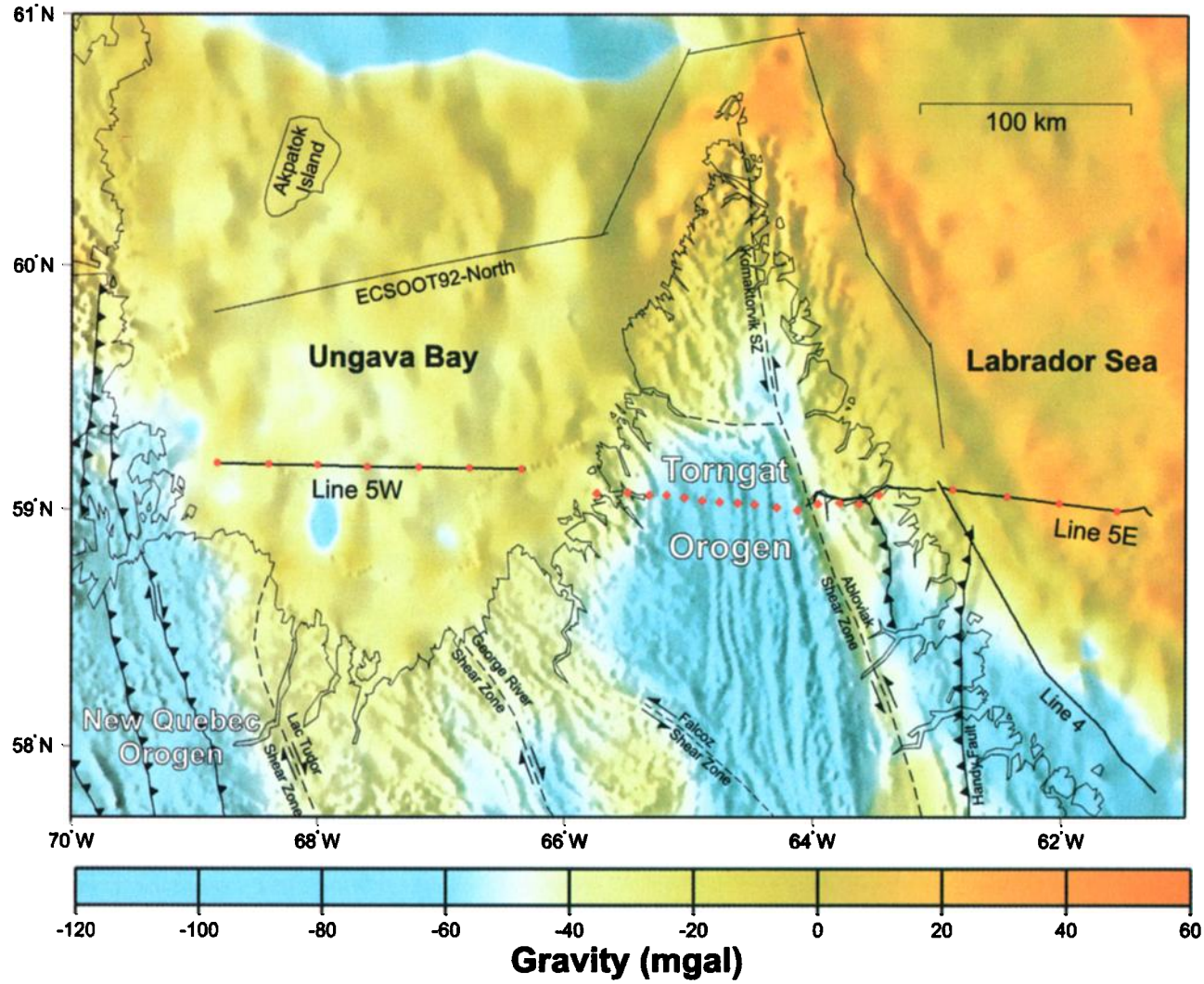

Plate 1. Gravity map around the transect area. Values on land are Bouguer anomalies and in offshore areas are free-air anomalies. The gray shading is derived from illumination of the magnetic anomalies from the west. Data courtesy of Geological Survey of Canada. Bold solid lines show the segments with airgun-shots; red circles and diamonds indicate the location of OBS and seismic land stations, respectively. Thin solid lines show the location of other seismic studies relevant to this study, as mentioned in the text. Solid lines with triangles mark faults and thrusts, dashed lines show shear zones (SZ), and arrows indicate the sense of displacement.

divided into two blocks, one west of 338 km with a fixed density of 3315 kg/m^3 and the other one to the east where density was varied. In addition to the density contrast, the depth of the lower boundary of the model was varied as well. The minimum RMS error is ~13 mGal and plots on a curve with a density contrast of 110 kg/m^3 for a lower boundary depth of 54 km, decreasing to a contrast of 65 kg/m^3 for a depth 85 km. To decide which point on this curve is most likely, additional information is necessary. It is likely that this deep density contrast is related to formation of the Labrador basin beginning in the Cretaceous. Because the Labrador basin has shallow basement depths and high heat flow with respect to standard oceanic lithospheric models [*Louden et al.*, 1989], its deeper mantle temperatures and densities must also be anomalous. These differences are probably related to hot spot activity, but we do not know how deep they extend. However, exact values of mantle density and thickness are not important as long as they fall along the minimum curve of the RMS error, and we arbitrarily assume a thickness of 60 km and density difference of 95 kg/m^3 (Figure 14).

Comparison between the observed and calculated gravity shows a reasonable agreement (Figure 14). Some minor misfit occurs in the westernmost 75 km, where the velocity model is associated with a higher uncertainty and where the model has no ray coverage. Calculated anomalies associated with the crustal root are up to 25 mGal too high, showing that there is a more complex transition in mantle density than can modeled by our simple approach with two constant density blocks in the mantle. In addition, some three-dimensional effects are likely. Despite these long-wavelength misfits, there is a very good agreement to the short-wavelength variations, indicating that features such as the crustal steps at the western border of the shear zone are consistent with the gravity data.

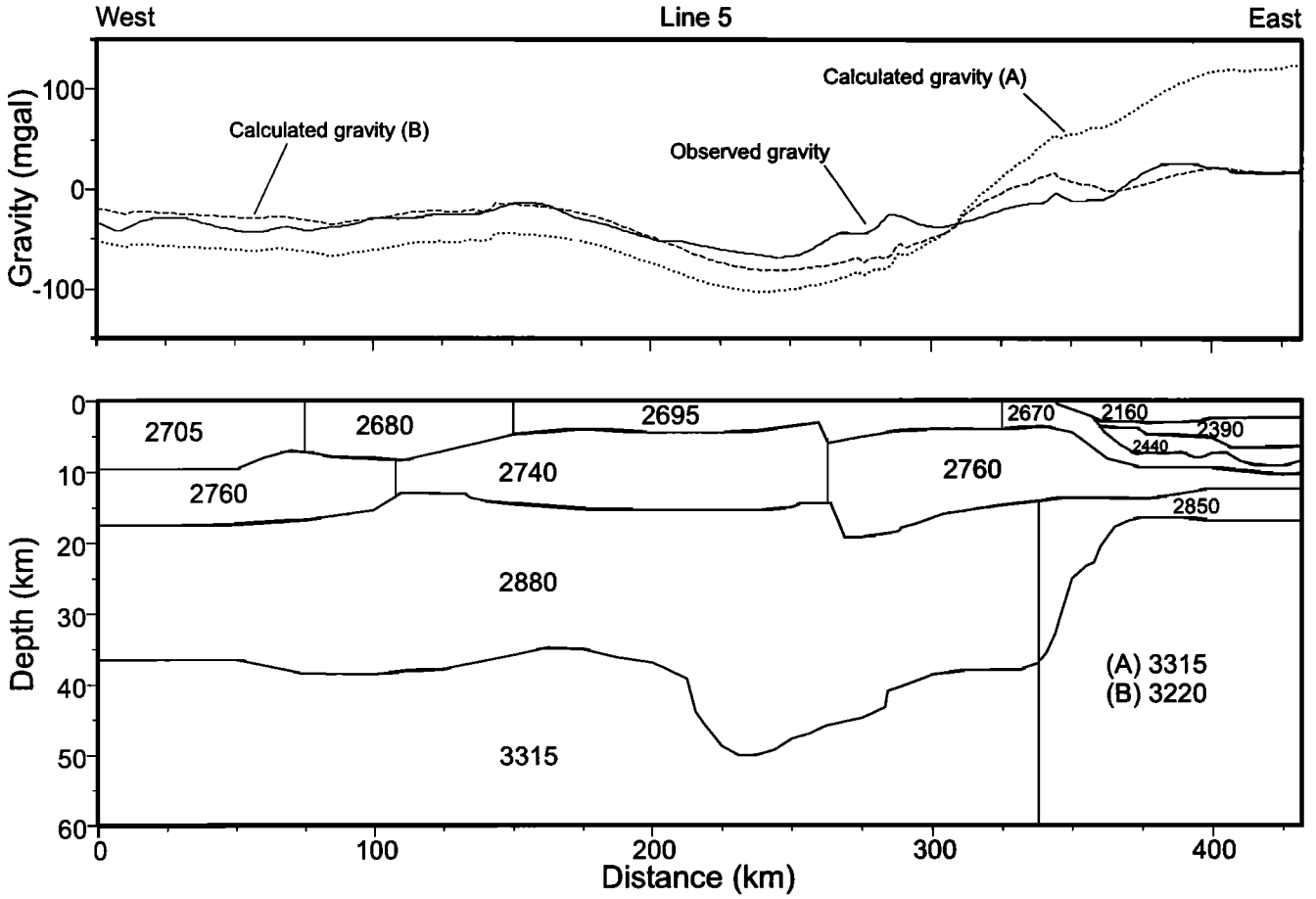

Figure 14. Two-dimensional gravity modeling for the transect line 5W-5E. The velocity model (Figure 12) was converted to a density model (model A), with values given in kg/m^3 using the velocity-density relationship of *Ludwig et al.* [1970]. For model B, the density in the mantle beneath the thinned crust was reduced. Observed gravity (solid line), and calculated gravity for model A (dotted line) and model B (dashed line) are shown in the top. Vertical exaggeration is 2.5.

5. Discussion

The following discussion will focus on the correlation of the velocity model (Figure 13) with the surface geology, and in particular on the implications for tectonic styles of deformation.

5.1. Core Zone

The Core Zone west of the Torngat Orogen has a fairly homogeneous structure, as indicated by the simplicity of its phase arrivals P_g, P_c, and P_mP (Figure 3). The velocity model of line 5 results in Moho two-way travel times (TWT) of 11-12 s with a westward dip. Moho depths on the ECSOOT 1992 reflection line [*Hall et al.*, 1995] of ~11.5 to 12.5 s TWT with a gentle westward dip are compatible with our model.

Features in the Core Zone that differ from the homogeneous structure include the slight domal uplifts at midcrustal levels (Figure 13), identified by reflections from the MCB (at ~120 km) and from the upper-/middle-crust boundary (at ~70 km). There are several interpretations for these structures. One is that they are related to offshore continuations of shear zones in that area. The patterns of the magnetic anomalies (Plate 1) do support at least some continuation of the shear zones into Ungava Bay, although the resolution of the magnetic data deteriorates substantially in the offshore area. The Lac Tudor shear zone at the eastern boundary of the New Quebec Orogen possibly intersects line 5W between OBS 2 and OBS 3, corresponding to a distance of 35 km along the line, and the George River shear zone could intersect the line at about 60 km. Hence both shear zones are possible candidates for the creation of the two reflective crustal uplift structures, assuming a generally eastward dip of crustal reflectivity as observed on the ECSOOT 1992 reflection profile [*Hall et al.*, 1995]. Even if there is no general relation to the large-scale shear zones, both features might be related to a single fault or crustal discontinuity that cuts through the middle crust with an eastward dip.

There is also the possibility that the reflector between the upper and middle crust is a more continuous feature than mapped by our survey. The low signal-to-noise ratio at the OBS recordings on line 5W might have prevented its detection. An argument against a continuous reflector is the lack of similar reflections on the ECSOOT 1992 reflection profile [*Hall et al.*, 1995] at the corresponding two-way travel time (TWT) of 2.5-3.0 s.

5.2. Torngat Orogen

Two important results of the velocity model are the existence of a crustal root beneath the orogen and the offset of the crust with vertical displacements of up to 5 km in the area of the Abloviak shear zone. The west-east extent of the crustal root is ~75 km, from 210 to 285 km along line 5. The north-south extent can only be estimated based on 2-D gravity modeling. The good correlation between the crustal root and the observed Bouguer gravity low (Figure 14 and Plate 1), suggests that the root may extend ~200 km from north to south. Consistent with this interpretation, we note that the ECSOOT 1992 reflection profile [*Hall et al.*, 1995] crosses the Torngat Orogen north of the gravity low and did not observe a crustal root beneath the orogen.

The velocity model of the Torngat Orogen on line 5 raises two major questions. (1) Which geodynamic interpretation can best explain the creation of the crustal structure beneath the Torngat Orogen? (2) How could the root be preserved for 1.7 Gyr, the time when the major deformation associated with the collision between the Nain and Superior cratons came to an end?

5.2.1. Geodynamic interpretation. The Torngat Orogen can be subdivided into two lateral segments. The northern Torngat Orogen (north of the Abloviak shear zone) is interpreted to result from eastward dipping subduction, with the 1910-1885 Ma suite of magmatic rocks in the Burwell domain representing a magmatic arc and the metasedimentary gneisses of the Tasiuyak domain interpreted as an accreted complex [*Van Kranendonk and Wardle*, 1994]. In contrast, the subduction direction in the southern Torngat Orogen is uncertain. *Wardle and Van Kranendonk* [1996] note that both the Nain and Core Zone margins are intruded by a magmatic suite. This is interpreted to result from a flip in the direction of subduction with time or by a double subduction (both to the east and west). However, preliminary dating of magmatic intrusions [*Scott*, 1995] suggests that its age is too young to be an expression of westward dipping subduction of the Nain Province beneath the Core Zone, and, in consequence, *Scott* [1998] suggests eastward dipping subduction for both the northern and southern Torngat Orogen. Eastward dipping subduction also is inferred from neodymium isotopic evidence in the southern part of the orogen [*Emslie et al.*, 1994], which indicates the presence of juvenile crust beneath the Nain craton.

The final velocity model of line 5 (Figure 13) is used to discuss three different geodynamic models for the southern Torngat Orogen. They are summarized in Figure 15.

1. Model A (Figure 15a) represents a westward dipping subduction. This model fits best with the geometry of the layer boundaries, showing a consistent westward dip in the Nain Province with almost parallel MCB and Moho. The western flank of the crustal root around 220 km (letter A) is interpreted as the transition zone to which the subducted ocean crust was or still is attached. During the subsequent collision of the Core Zone and the Nain Province, the eastern block was overthrust by the western block. This model of overthrusting is consistent with the interpretation of *Hall et al.* [1995], who suggest that the strong reflectors at the base of the crust of the Core Zone indicate detachment of Core Zone crust from the underlying mantle. The offset in the lower and middle crust at 265 km (letters B and C) is interpreted to be related to the overthrusting and may also include shearing associated with the oblique convergence of the Nain and Superior cratons. In this scenario, the Moho offset at 285 km (letter D) is interpreted as a similar feature but one that is decoupled from the offsets at lower-and middle-crustal levels (letters B and C).

2. Model B (Figure 15b) with eastward dipping subduction can be explained only with difficulty by the geometry of the velocity model. This includes the fact that the subducted slab (letter E) dips very steeply under the Nain block and is located almost entirely to the west of the axial zone of the Torngat Orogen, which is located near the Tasiuyak domain and Lac Lomier complex [*Wardle and Van Kranendonk*, 1996]. In case of eastward dipping subduction, the shape of the western flank of the crustal root would be expected to be upward convex (letter F) rather than downward convex (letter G) as in the final velocity model. Another problem arising with eastward subduction is the coherent reflections from the Moho segment between 240 and 280 km (letter H). This section of the Moho would correspond to the slab breakoff, and a coherent reflection from this zone is therefore rather improbable. In contrast, the arrangement of the crustal offsets (letters B, C, and D) as eastward dipping features can be explained well with model B. Mechanically weak crust that is squeezed between stronger crustal units tends to focus strain [*Ellis and Beaumont*, 1996] such as that associated with the oblique convergence of the Nain and Superior cratons which resulted in the major shear zones. Such a comparatively weak unit would exist between the Core Zone and Nain crust (probably to the base of the crust), where the Tasiuyak metasediments have been accreted during the subduction

3. Model C (Figure 15c) is an attempt to explain the crustal root without requiring that it represents any subducted crustal slab. In this model, the root is formed as consequence of the oblique collision of the two crustal blocks (Core Zone and Nain) and the associated transpressional stress regime. The observed geological surface structures are explained by flower structures originating from the crustal root (letter J). Problems with this model include an explanation for the asymmetry in the crustal root and the location of the root to the west of the axial zone of the orogen

In summary, model C seems least likely in view of the geometric considerations. Model A with westward subduction shows a better agreement with the surface geology and velocity model of the lower crust and mantle than model B with eastward subduction. Given the geochemical evidence for eastward dipping subduction [*Emslie et al.*, 1994], the present geometry may represent a later stage of the collision dynamics. This model would imply a flip of subduction direction. Alternatively, model A can be modified to a scenario of late westward underthrusting of Nain crust as opposed to subduction. This underthrusting might be associated with easterly directed thrusting between 1.8 and 1.74 Ga [*Van Kranendonk*, 1996]. These thrusts are later than the Abloviak shear zone and may be displacing it to lower crustal levels.

5.2.2. Preservation of the crustal root. The preservation of a crustal root beneath the Torngat Orogen for 1.7 Ga is surprising. The Wilson cycle [*Wilson*, 1966] suggests erosion of mountain belts and corresponding disappearance of crustal roots over cycles of ~500 Myr. In proximity to line 5, there is reported to be a normal thickness in the northern Torngat Orogen [*Hall et al.*, 1995]. To the south in the Labradorian Orogen (Grenville Province; Figure 1) a reduced crustal thickness was interpreted from seismic and gravity data [*Gower et al.*, 1997; *Louden and Fan*, 1998].

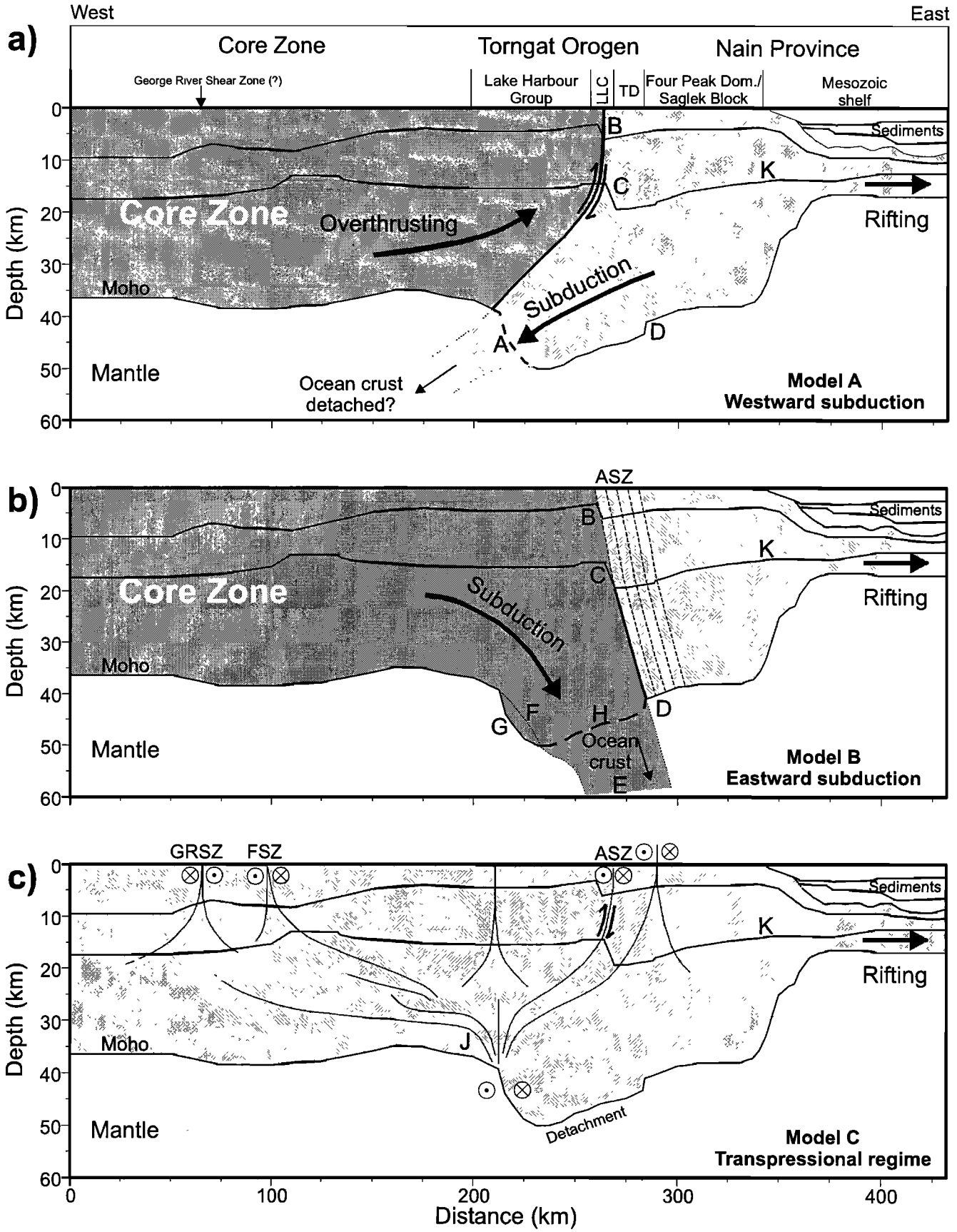

Figure 15. Geodynamical interpretation of the seismic transect superimposed on the velocity model shown in Figure 13. The crustal root is interpreted as a feature caused (a) by westward dipping subduction of the Nain Province, (b) by eastward dipping subduction of the Core Zone, or (c) by the transpressional stress regime. Arrows indicate the sense of motion/displacement, and dotted and crossed circles refer to motion out of and into the two-dimensional plain, respectively. Letters in the model refer to features discussed in the text. Tectonic units are indicated above the individual models. Abbreviations are LLC, Lac Lomier complex; TD, Tasiuyak domain; Dom, Domain; ASZ, Abloviak shear zone; GRSZ, George River shear zone; and FSZ, Falcoz shear zone. Vertical exaggeration is 2.6.

Although crustal roots beneath Proterozoic and also Paleozoic orogens are atypical, there are at least a few other examples of roots. Beneath the Bothnian Bay in the Baltic Shield, the *BABEL Working Group* [1990] found a root with a Moho depth of ~55 km. *P*-wave velocities in this root are as high as 7.7 km/s [*BABEL Working Group*, 1993]. Beneath the Proterozoic Trans-Hudson Orogen in central Canada, Moho depth at the crustal root is up to 52 km [*Németh et al.*, 1996; *Lucas et al.*, 1993]. In the Paleozoic Uralide Orogen, *Carbonell et al* [1996] reported a 12- to 15-km-thick crustal root and a total crustal thickness of 55-58 km. Explanations for the preservation of these roots vary. *Berzin et al.* [1996] suggest that the Urals did not experience significant postorogenic collapse and that they possibly evolved isostatically and never existed as a gravitationally unstable belt of high topography. The preservation of a root beneath the Bothnian Bay is explained by the lack of strong heating and deformation of the lower crust and uppermost mantle since the formation of the Moho offset [*BABEL Working Group*, 1990]. *Lucas et al* [1996] interpret the short-wavelength Moho topography (including the root) in the Trans-Hudson Orogen as result of variable ductile reworking of the lower crust during postcollisional deformation.

For the Torngat Orogen, we favor an explanation similar to the one given for the Baltic shield, which is the absence of postorogenic heating and ductile reworking. This lack of heating in the southern Churchill Province agrees with the lack of abundant postcollisional granitoid magmatism. The juvenile crustal elements of the southeastern Churchill Province have been largely underlain by Archean lithosphere, the depleted and refractory nature of which may have inhibited large-scale crustal melting during postcollisional delamination/slab-breakoff and uplift [cf. *von Blanckenburg and Davies*, 1995]. The lack of a high-velocity zone in the lower crust of the Torngat Orogen supports the theory that there was no substantial underplated melt.

5.3. Nain Province

In the western part of the Nain Province, the crust adjacent to the Torngat Orogen has a thickness similar to the Core Zone. There is a slight westward dip to the layer boundaries up to a distance of 338 km where thinning of the crust starts (letter K in Figure 15). Velocities in the unstretched portion of the crust are comparable to those found on the cross line (ECSOOT line 4 [*Funck and Louden*, 1998]) parallel to the coast of Labrador (Figure 2), where the Moho depth varies between 33 and 38 km.

For the cross line, *Funck and Louden* [1998] inferred from the *P*- and *S*-wave velocity structure a felsic composition for the upper and middle crust and an intermediate character of the lower crust. This interpretation is confirmed for line 5 by the measurement of *P*- and *S*-wave velocities under various pressure conditions for rock samples collected along the Nachvak Fjord on line 5E (M.H. Salisbury and A.M. Muzzatti, personal communication, 1998). Velocities in the upper and middle crust (5.9-6.55 km/s) agree best with rock samples having a felsic-gneiss lithology. For the lower crust (6.65-6.90 km/s), felsic gneiss samples have velocities that are too low, whereas the mafic gneisses are in general too fast. An intermediate composition of the lower crust seems therefore to be most likely.

The thinned crust east of 335 km (letter K in Figure 15) is interpreted to be stretched continental crust. This is in agreement with the interpretation of magnetic anomalies in the Labrador Sea, showing the ocean-continent boundary ~175 km off the present coast line [*Roest and Srivastava*, 1989] or ~80 km farther offshore than the eastern limit of line 5E. *Chian et al.* [1995] show that the Labrador margin to the south has a ~140-km-wide zone with typical continental crust velocities, associated with deeply subsided and stretched continental crust [*Chian et al.*, 1995]. This description is similar to the crustal structure on line 5E (Figure 13), but thinning occurs more rapidly. The crust is reduced from a thickness of 38 km in the pristine Nain Province to a residual thickness of only 9 km, and it has subsided by about 8 km beneath the sediment load. The velocities in the 9-km-thick crust range from 5.8 to 6.75 km/s, which are typical of the original continental velocities.

On the Labrador margin, no underplated zone has been observed [*Chian et al.*, 1995]. Consistent with that observation, no high-velocity zone (HVZ) is observed at the base of the crust on line 5E over the entire 100 km offshore of the coastline covered by the experiment. This result is contrary to the conjugate portion of the Greenland margin, where *Gohl and Smithson* [1993] reported a HVZ in the lowermost crust, with a maximum thickness of 8 km and velocities between 7.4 and 7.8 km/s, that they interpreted as an underplated igneous complex. Farther south at the SW Greenland margin, *Chian and Louden* [1992] did not observe any HVZ in the lower crust. The lack of any underplating on line 5E supports the interpretation of *Gohl and Smithson* [1993] that the HVZ at the conjugate margin of Greenland might be related to active rifting to the north of Davis Strait and Baffin Bay due to hot spot activity. In this case, the underplating must have occurred following the initial opening of the Labrador Sea.

6. Conclusions

The west-east seismic transect on line 5 reveals a ~50-km-deep crustal root with a width of about 75 km beneath the Paleoproterozoic Torngat Orogen. Two-dimensional gravity modeling indicates that the crustal root correlates with a gravity low that extends up to 100 km from west to east and ~200 km from north to south. On the basis of this correlation, the crustal root does not extend across the Abloviak shear zone into the northern Torngat Orogen, which is in agreement with a reflection seismic line in that area [*Hall et al.*, 1995].

General westward dipping layer boundaries in the Nain Province and beneath the Torngat Orogen suggest that the crustal root was formed either (1) by westward dipping subduction of Nain crust beneath the Core Zone following early eastward dipping subduction of Core Zone crust beneath the Nain block or (2) by westward underthrusting of Nain crust in a late stage of the collision. The preservation of the crustal root over a period of ~1.8 Gyr is rather unusual, although other examples are known from closely related Paleoproterozoic orogens in the Baltic shield [*BABEL Working Group*, 1990] and the Trans-Hudson Orogen [*Németh et al.*, 1996]. We attribute the preservation of the crustal root beneath the Torngat Orogen to the absence of postorogenic heating and ductile reworking. This interpretation is in agreement with the lack of abundant postcollisional magmatism in the SE Churchill Province.

The combination of dense shot spacing (<150 m) and dense receiver spacing onshore (~9 km) has enabled a detailed image of the crustal velocity structure to be determined, allowing us to detect the discontinuity at the Abloviak shear zone already at upper crustal levels. The correlation of this discontinuity down to the Moho shows that the associated transcurrent shearing is a major feature that affects the entire crust. Another fault cutting through the crust down to the mantle was found on line 4 (Figure 2), close to the transect in the Nain Province [*Funck and Louden*, 1998]. The preservation of fault offsets at Moho level is further evidence of the lack of postorogenic heating and reworking at lower crustal level.

Acknowledgments. We thank Ian Reid and other participants of CSS *Hudson* cruise 96-021 and of the land operations, who helped to carry out the seismic experiment. Mike Gorveatt helped with cruise preparations and logistics, and Bruce Mitchell assisted in the processing of the data. We also thank Jeremy Hall and Richard Wardle for their helpful comments on this paper. John McBride, Gerald Ross, and Tim Henstock are thanked for their detailed and helpful reviews. The Geophysical DataCentre, Geological Survey of Canada, supplied the gravity and magnetic data. Judith McIntyre of the Canada-Newfoundland Offshore Petroleum Board made the industry data available to us. This work was supported by the Lithoprobe program of the Natural Science and Engineering Research Council of Canada and Geological Survey of Canada.This is Lithoprobe contribution 1013.

References

BABEL Working Group, Evidence for Precambrian plate tectonics from seismic profiling in the Baltic Shield, *Nature, 348*, 34-38, 1990.

BABEL Working Group, Integrated seismic studies of the Baltic shield using data in the Gulf of Bothnia region, *Geophys. J. Int., 112*, 305-324, 1993.

Bertrand, J.-M., J.C. Roddick, M.J. Van Kranendonk, and I. Ermanovics, U-Pb geochronology of deformation and metamorphism across a central transect of the Early Proterozoic Torngat Orogen, North River map area, Labrador, *Can. J. Earth Sci., 30*, 1470-1489, 1993.

Berzin, R., O. Oncken, J.H. Knapp, A. Pérez-Estaún, T. Hismatulin, N. Yunusov, and A. Lipilin, Orogenic evolution of the Ural mountains: Results from an integrated seismic experiment, *Science, 274*, 220-221, 1996.

Bridgwater, D., and L. Schiøtte, The Archean gneiss complex of northern Labrador: A review of current results, ideas and problems, *Bull. Geol. Soc. Den., 39*, 153-166, 1991.

Bridgwater, D., and R.J. Wardle, Whole rock Pb isotopic compositions of Archean and Proterozoic rocks from northern Labrador used to separate major units in the shield, in *Eastern Canadian Shield Onshore-Offshore Transect (ECSOOT), Report of Transect Meeting, Lithoprobe Rep., 32*, edited by R.J. Wardle and J. Hall, pp. 42-51, Univ. of B.C., Vancouver, Canada, 1992.

Bridgwater, D., A. Escher, and J. Watterson, Tectonic displacement and thermal activity in two contrasting Proterozoic mobile belts from Greenland, *Philos. Trans. R. Soc. London, Ser. A, 273*, 513-533, 1973.

Carbonell, R., A. Pérez-Estaún, J. Gallart, J. Diaz, S. Kashubin, J. Mechie, R. Stadtlander, A. Schulze, J.H. Knapp, and A. Morozov, Crustal root beneath the Urals: Wide-angle seismic evidence, *Science, 274*, 222-224, 1996.

Chian, D., and K.E. Louden, The structure of Archean-Ketilidian crust along the continental shelf of southwestern Greenland from a seismic refraction profile, *Can. J. Earth Sci., 29*, 301-313, 1992.

Chian, D., C. Keen, I. Reid, and K. Louden, Evolution of nonvolcanic rifted margins: New results from the conjugate margins of the Labrador Sea, *Geology, 23*, 589-592, 1995.

Dunphy, J.M., and T. Skulski, Early Proterozoic granitic magmatism in the Ungava and New Quebec orogens:The Narsajuaq Terrane and the De Pas Batholith, in *Eastern Canadian Shield Onshore-Offshore Transect (ECSOOT), Report of Transect Meeting, Lithoprobe Rep., 45*, edited by R.J. Wardle and J. Hall, pp. 37-50, Univ. of B.C., Vancouver, Canada, 1995.

Ellis, S., and C. Beaumont, Models of convergent boundary tectonics: Implications for the interpretation of Lithoprobe data, in *Eastern Canadian Shield Onshore-Offshore Transect (ECSOOT), Report of Transect Meeting, Lithoprobe Rep., 57*, edited by R.J. Wardle and J. Hall, pp. 59-108, Univ. of B.C., Vancouver, Canada, 1996.

Emslie, R.F., M.A. Hamilton, and R.J. Thériault, Petrogenesis of a mid-Proterozoic anorthosite - mangerite - charnockite - granite (AMCG) complex: Isotopic and chemical evidence from the Nain Plutonic Suite, *J. Geol., 102*, 539-558, 1994.

Ermanovics, I., and M. Van Kranendonk, The Torngat Orogen in the North River - Nutac transect of Nain and Churchill provinces, *Geosci. Can., 17*, 279-283, 1990.

Funck, T., and K.E. Louden, Wide-angle seismic imaging of pristine Archean crust in the Nain Province, Labrador, *Can. J. Earth Sci., 35, 672-685*, 1998.

Gohl, K., and S.B. Smithson, Structure of Archean crust and passive margin of southwest Greenland from seismic wide-angle data, *J. Geophys. Res., 98*, 6623-6638, 1993.

Goulet, N., and A. Ciesielski, The Abloviak Shear Zone and the NW Torngat Orogen, eastern Ungava Bay, Québec, *Geosci. Can., 17*, 269-272, 1990.

Gower, C.F., J. Hall, G.J. Kilfoil, G.M. Quinlan, and R.J. Wardle, Roots of the Labradorian orogen in the Grenville Province in southeastern Labrador: Evidence from marine, deep-seismic reflection data, *Tectonics, 16*, 795-809, 1997.

Hall, J., R.J. Wardle, C.F. Gower, A. Kerr, K. Coflin, C.E. Keen, and P. Carroll, Proterozoic orogens of the northeastern Canadian Shield: New information from the Lithoprobe ECSOOT crustal reflection seismic survey, *Can. J. Earth Sci., 32*, 1119-1131, 1995.

Jackson, G.D., and F.C. Taylor, Correlation of major Aphebian rock units in the northeastern Canadian Shield, *Can. J. Earth Sci, 9*, 1659-1669, 1972.

James, D.T., J.N. Connelly, H.A. Wasteneys, and G.J. Kilfoil, Paleoproterozoic lithotectonic subdivisions of the southeastern Churchill Province, western Labrador, *Can. J. Earth Sci., 33*, 216-230, 1996.

Louden, K.E., and J. Fan, Crustal structure of Grenville, Makkovik, and southern Nain provinces along the Lithoprobe ECSOOT Transect: Regional seismic refraction and gravity models and their tectonic implications, *Can. J. Earth Sci., 35*, 583-601, 1998.

Louden, K.E., K.A. Dadey, and S.P Srivastava, Heat-flow measurements at Hole 646A, *Proc. Ocean Drill. Program Sci. Results, 105*, 923-931, 1989.

Lucas, S.B., A. Green, Z. Hajnal, D. White, J. Lewry, K. Ashton, W. Weber, and R. Clowes, Deep seismic profile across a Proterozoic collision zone: Surprise at depth, *Nature, 363*, 339-342, 1993.

Ludwig, W.J., J.E., Nafe, and C.L. Drake, Seismic refraction, in *The Sea*, edited by A.E. Maxwell, pp. 53-84, Wiley-Intersci., New York, 1970.

Németh, B., Z. Hajnal, and S.B. Lucas, Moho signature from wide-angle reflections: Preliminary results of the 1993 Trans-Hudson orogen refraction experiment, *Tectonophysics, 264*, 111-121, 1996.

Perreault, S., and A. Hynes, Tectonic evolution of the Kuujjuac terrane, New Québec Orogen, *Geosci. Can., 17*, 238-240, 1990.

Rivers, T., F. Mengel, D.J. Scott, L.M. Campbell, and N. Goulet, Torngat Orogen - A Palaeoproterozoic example of a narrow doubly vergent collisional orogen, in *Precambrian Crustal Evolution in the North Atlantic Region*, edited by T.S. Brewer, *Spec. Publ., Geol. Soc. London, 112*, 117-136, 1996.

Roest, W.R., and S.P. Srivastava, Sea-floor spreading in the Labrador Sea: A new reconstruction, *Geology, 17*, 1000-1003, 1989.

Scott, D.J., U-Pb geochronology of the northeastern Rae Province,I, A preliminary report on the Lac Lomier complex, northern Labrador, in *Eastern Canadian Shield Onshore-Offshore Transect (ECSOOT), Report of Transect Meeting, Lithoprobe Rep., 45*, edited by R.J. Wardle and J. Hall, pp. 122-128, Univ. of B.C., Vancouver, Canada, 1995.

Scott, D.J., An overview of the U-Pb geochronology of the Paleoproterozoic Torngat Orogen, northeastern Canada, *Precambrian Res., 91*, 91-107, 1998.

Srivastava, S.P., Evolution of the Labrador Sea and its bearing on the early evolution of the North Atlantic,*Geophys. J. R Astron. Soc., 52*, 313-357, 1978.

Sutton, J.S., B.E. Marten, A.M.S. Clark, and I. Knight, Correlation of the Precambrian supracrustal rocks of coastal Labrador and southwest Greenland, *Nature, 238*, 122-123, 1972.

Van Kranendonk, M.J., Tectonic evolution of the Paleoproterozoic Torngat Orogen: Evidence from pressure-temperature-time-deformation paths in the North River map area, Labrador,*Tectonics, 15*, 843-869, 1996.

Van Kranendonk, M.J., and R.J. Wardle, Geological synthesis and musings on possible subduction-accretion models in the formation of the northern Torngat Orogen, in *Eastern Canadian Shield Onshore-Offshore Transect (ECSOOT), Report of Transect Meeting, Lithoprobe Rep., 36*, edited by R.J. Wardle and J. Hall, pp. 62-80, Univ. of B.C., Vancouver, Canada, 1994.

Van Kranendonk, M.J., R.J. Wardle, F.C. Mengel, L.M. Campbell, and L. Reid, New results and summary of the Archean and Paleoproterozoic geology of the Burwell domain, northern Torngat Orogen, Labrador, Quebec and Northwest Territories, in *Current Research, Part C, Geol. Surv. Can., Pap. 94-1C*,321-332, 1994.

von Blanckenburg, F., and J.H. Davies, Slab breakoff: A model for syncollisional magmatism and tectonics in the Alps,*Tectonics, 14*, 120-131, 1995.

Wardle, R.J., and M.J. Van Kranendonk, The Palaeoproterozoic southeastern Churchill Province of Labrador-Quebec, Canada: Orogenic development as a consequence of oblique collision and indentation, in *Precambrian Crustal Evolution in the North Atlantic Region*, edited by T.S. Brewer, *Spec. Publ, Geol. Soc. London, 112*, 137-153, 1996.

Wares, R.P. and J. Goutier, Deformation style in the foreland of the New Quebec Orogen, *Geosci. Can., 17*, 244-249, 1990.

Wilson, J.T., Did the Atlantic close and then re-open?,*Nature, 211*, 676-681, 1966.

Zelt, C.A., and R.M. Ellis, Practical and efficient ray tracing in two-dimensional media for rapid travel time and amplitude forward modelling, *Can. J. Explor. Geophys., 24*, 16-31, 1988.

Zelt, C.A., and D.A. Forsyth, Modeling wide-angle seismic data for crustal structure: Southeastern Grenville Province, *J. Geophys. Res., 99*, 11,687-11,704, 1994.

Zelt, C.A., and R.B. Smith, Seismic travel time inversion for 2-D crustal velocity structure. *Geophys. J. Int., 108*, 16-34, 1992.

T. Funck and K. Louden, Department of Oceanography, Dalhousie University, Halifax, Nova Scotia, Canada, B3H 4J1. (tfunck@is.dal.ca)

(Received May 18, 1998; revised December 9, 1998; accepted January 6, 1999.)